

Optimistic limits of the colored Jones polynomials

JINSEOK CHO AND JUN MURAKAMI

August 7, 2012

Abstract

We show that the optimistic limits of the colored Jones polynomials of the hyperbolic knots coincide with the optimistic limits of the Kashaev invariants modulo $4\pi^2$.

1 Introduction

1.1 Preliminaries

Kashaev conjectured the following relation in [4] :

$$\text{vol}(L) = 2\pi \lim_{N \rightarrow \infty} \frac{\log |\langle L \rangle_N|}{N},$$

where L is a hyperbolic link, $\text{vol}(L)$ is the hyperbolic volume of $S^3 - L$, and $\langle L \rangle_N$ is the N -th Kashaev invariant. After that, the generalized conjecture was proposed in [11] that

$$i(\text{vol}(L) + i \text{cs}(L)) \equiv 2\pi i \lim_{N \rightarrow \infty} \frac{\log \langle L \rangle_N}{N} \pmod{\pi^2},$$

where $\text{cs}(L)$ is the Chern-Simons invariant of $S^3 - L$ defined in [6].

The calculation of the actual limit of the Kashaev invariant is very hard, and only several cases are known. On the other hand, while proposing the conjecture, Kashaev used some formal approximation to predict the actual limit. His formal approximation was formulated as *optimistic limit* by H. Murakami in [8]. This method can be summarized by the following way. At first, we fix an expression of $\langle L \rangle_N$ and then apply the following *formal substitution*

$$\begin{aligned} (q)_k &\sim \exp \left\{ \frac{N}{2\pi i} \left(-\text{Li}_2(q^k) + \frac{\pi^2}{6} \right) \right\}, \\ (q^{-1})_k &\sim \exp \left\{ \frac{N}{2\pi i} \left(\text{Li}_2(q^{-k}) - \frac{\pi^2}{6} \right) \right\}, \\ q^{kl} &\sim \exp \left\{ \frac{N}{2\pi i} (\log q^k \cdot \log q^l) \right\}, \end{aligned} \tag{1}$$

to the expression, where $q = \exp(2\pi i/N)$, $\text{Li}_2(z) = -\int_0^z \frac{\log(1-t)}{t} dt$ for $z \in \mathbb{C}$, $[k]$ is the residue of an integer k modulo N , $(q)_k = \prod_{n=1}^{[k]} (1 - q^n)$ and $(q)_0 = 1$. Then, by substituting each q^k with a complex variable z , we obtain a potential function $\exp\left\{\frac{N}{2\pi i} F(\dots, z, \dots)\right\}$. Finally, let

$$F_0(\dots, z, \dots) := F - \sum_z \left(z \frac{\partial F}{\partial z} \right) \log z$$

and evaluate F_0 for an *appropriate solution* of the equations $\{\exp(z \frac{\partial F}{\partial z}) = 1\}$. Then, the resulting complex number is called *the optimistic limit*.

For example, the optimistic limit of the Kashaev invariant of the 5_2 knot was calculated in [4] and [12] as follows. By the formal substitution,

$$\langle 5_2 \rangle_N = \sum_{k \leq l} \frac{(q)_l^2}{(q^{-1})_k} q^{-k(l+1)} \sim \exp \left\{ \frac{N}{2\pi i} \left(-2\text{Li}_2(q^l) - \text{Li}_2\left(\frac{1}{q^k}\right) - \log q^l \log q^k + \frac{\pi^2}{2} \right) \right\}.$$

By substituting $z = q^l$ and $u = q^k$, we obtain

$$F(z, u) = -2\text{Li}_2(z) - \text{Li}_2\left(\frac{1}{u}\right) - \log z \log u + \frac{\pi^2}{2},$$

and

$$F_0(z, u) = F(z, u) - \left(z \frac{\partial F}{\partial z} \right) \log z - \left(u \frac{\partial F}{\partial u} \right) \log u.$$

For the choice of a solution $(z_0, u_0) = (0.3376... - i 0.5623..., 0.1226... + i 0.7449...)$ of the equations $\{\exp(z \frac{\partial F}{\partial z}) = 1, \exp(u \frac{\partial F}{\partial u}) = 1\}$, the optimistic limit becomes

$$F_0(z_0, u_0) = i(2.8281... - i 3.0241...) \equiv i(\text{vol}(5_2) + i \text{cs}(5_2)) \pmod{\pi^2}.$$

As seen above, the optimistic limit depends on the expression and the choice of the solution, so it is not well-defined. However, Yokota made a very useful way to determine the optimistic limit of a hyperbolic knot K , in [16] and [17], by defining a potential function $V(z_1, \dots, z_g)$ of the knot diagram, which also comes from the formal substitution of certain expression of the Kashaev invariant $\langle K \rangle_N$. (The definition of $V(z_1, \dots, z_g)$ will be in Section 3.1.) As above, he also defined

$$V_0(z_1, \dots, z_g) := V - \sum_{k=1}^g \left(z_k \frac{\partial V}{\partial z_k} \right) \log z_k,$$

and

$$\mathcal{H}_1 := \left\{ \exp\left(z_k \frac{\partial V}{\partial z_k}\right) = 1 \mid k = 1, \dots, g \right\}.$$

After proving \mathcal{H}_1 is the hyperbolicity equation of Yokota triangulation, he chose the geometric solution $\mathbf{z}^{(0)} = (z_1^{(0)}, \dots, z_g^{(0)})$ of \mathcal{H} . (Yokota triangulation will be in Section 2.1. The hyperbolicity equation consists of edge relations and the cusp conditions of a triangulation, and

the geometric solution is the one which gives the hyperbolic structure of the triangulation. Details will be in Section 4.) Then he proved

$$V_0(\mathbf{z}^{(0)}) \equiv i(\text{vol}(K) + i \text{cs}(K)) \pmod{\pi^2}, \quad (2)$$

in [17]. Therefore, we denote

$$2\pi i \text{ o-lim}_{N \rightarrow \infty} \frac{\log \langle K \rangle_N}{N} := V_0(\mathbf{z}^{(0)}),$$

and call it *the optimistic limit of the Kashaev invariant* $\langle K \rangle_N$.

To obtain (2), Yokota assumed several assumptions of the knot diagram and the existence of an essential solution of \mathcal{H}_1 . The assumptions of the diagram roughly mean to reduce redundant crossings of the diagram before finding the potential function V . Exact statements are **Assumption 1.1–1.4.** and **Assumption 2.2.** in [17]. We remark that these assumptions are needed so that, after the collapsing process, Yokota triangulation becomes a topological triangulation of the knot complement $S^3 - K$. (See Section 3.1 for details.)

As mentioned before, the set of equations \mathcal{H}_1 becomes the hyperbolicity equation of Yokota triangulation. Therefore, each solution $\mathbf{z} = (z_1, \dots, z_g)$ of \mathcal{H}_1 determines the shape parameters of the ideal tetrahedra of the triangulation and the parameters are expressed by the ratios of z_1, \dots, z_g . (Details are in Section 4.) We call a solution \mathbf{z} of \mathcal{H}_1 *essential* if no shape parameters are in $\{0, 1, \infty\}$, which implies no edges of the triangulation are homotopically nontrivial. A well-known fact is that if the hyperbolicity equation has an essential solution, they have the geometric solution $\mathbf{z}^{(0)}$ of \mathcal{H}_1 . (For details, see Section 2.8 of [15].) Therefore, to guarantee the existence of the geometric solution, Yokota assumed the existence of an essential solution.

On the other hand, it was proved in [10] that

$$J_L(N; \exp \frac{2\pi i}{N}) = \langle L \rangle_N,$$

where $J_L(N; x)$ is the N -th colored Jones polynomial of the link L with a complex variable x . Therefore, it is natural to define the optimistic limit of the colored Jones polynomial so that it gives the volume and the Chern-Simons invariant. Although it looks trivial, due to the ambiguity of the optimistic limit, only few results were known. It was numerically confirmed for few examples in [11], actually proved only for the volume part of two bridge links in [12] and for the Chern-Simons part of twist knots in [2]. In a nutshell, the purpose of this article is to propose a general method to define the optimistic limit of the colored Jones polynomial of a hyperbolic knot K and then to prove the following relation :

$$2\pi i \text{ o-lim}_{N \rightarrow \infty} \frac{\log \langle K \rangle_N}{N} \equiv 2\pi i \text{ o-lim}_{N \rightarrow \infty} \frac{\log J_K(N; \exp \frac{2\pi i}{N})}{N} \pmod{4\pi^2}. \quad (3)$$

1.2 Main result

For a hyperbolic knot K , we define a potential function $W(w_1, \dots, w_m)$ of a knot diagram in Section 3.2, which also comes from the formal substitution of certain expression of the

colored Jones polynomial $J_L(N; \exp \frac{2\pi i}{N})$. We define

$$W_0(w_1, \dots, w_m) := W - \sum_{l=1}^m \left(w_l \frac{\partial W}{\partial w_l} \right) \log w_l,$$

and

$$\mathcal{H}_2 := \left\{ \exp \left(w_l \frac{\partial W}{\partial w_l} \right) = 1 \mid l = 1, \dots, m \right\}.$$

Also we discuss Thurston triangulation of the knot complement $S^3 - K$ in Section 2.2, which was introduced in [13].

Proposition 1.1. *For a hyperbolic knot K with a fixed diagram, we assume the diagram satisfies **Assumption 1.1–1.4.** and **Assumption 2.2.** in [17]. For the potential function $W(w_1, \dots, w_m)$ of the diagram, \mathcal{H}_2 becomes the hyperbolicity equation of Thurston triangulation.*

Proof of Proposition 1.1 will be in Section 4.

Each solution $\mathbf{w} = (w_1, \dots, w_m)$ of \mathcal{H}_2 determines the shape parameters of the ideal tetrahedra of Thurston triangulation and the parameters are expressed by the ratios of w_1, \dots, w_m . (Details are in Section 4.) We call a solution \mathbf{w} of \mathcal{H}_2 *essential* if no shape parameters are in $\{0, 1, \infty\}$. Comparing Yokota triangulation and Thurston triangulation, we obtain the following Lemma.

Lemma 1.2. *For a hyperbolic knot K with a fixed diagram, assume the assumptions of Proposition 1.1. Then an essential solution $\mathbf{z} = (z_1, \dots, z_g)$ of \mathcal{H}_1 determines the unique solution $\mathbf{w} = (w_1, \dots, w_m)$ of \mathcal{H}_2 , and vice versa. Furthermore, if the determined solution \mathbf{w} is essential, then \mathbf{w} induces \mathbf{z} too, and vice versa.*

Proof of Lemma 1.2 will be in Section 5. Although there is a possibility that an essential solution \mathbf{z} of \mathcal{H}_1 determines non-essential solution \mathbf{w} of \mathcal{H}_2 , we expect this does not happen for almost all cases. In this article, we only consider the case when the determined solution \mathbf{w} is essential.

Theorem 1.3. *For a hyperbolic knot K with a fixed diagram, assume the assumptions of Proposition 1.1. Let $V(z_1, \dots, z_g)$ and $W(w_1, \dots, w_m)$ be the potential functions of the knot diagram. Also assume the hyperbolicity equation \mathcal{H}_1 has an essential solution $\mathbf{z} = (z_1, \dots, z_g)$ and let $\mathbf{z}^{(0)} = (z_1^{(0)}, \dots, z_g^{(0)})$ be the geometric solution of \mathcal{H}_1 . From Lemma 1.2, let $\mathbf{w} = (w_1, \dots, w_g)$ and $\mathbf{w}^{(0)} = (w_1^{(0)}, \dots, w_m^{(0)})$ be the corresponding solutions of \mathcal{H}_2 determined by \mathbf{z} and $\mathbf{z}^{(0)}$ respectively. We also assume \mathbf{w} and $\mathbf{w}^{(0)}$ are essential. Then*

1. $V_0(\mathbf{z}) \equiv W_0(\mathbf{w}) \pmod{4\pi^2}$,
2. $\mathbf{w}^{(0)}$ is the geometric solution of \mathcal{H}_2 and

$$W_0(\mathbf{w}^{(0)}) \equiv i(\text{vol}(K) + i \text{cs}(K)) \pmod{\pi^2}.$$

The proof will be in Section 5. We denote

$$2\pi i \lim_{N \rightarrow \infty} \frac{\log J_K(N; \exp \frac{2\pi i}{N})}{N} := W_0(\mathbf{w}^{(0)}),$$

and call it *the optimistic limit of the colored Jones polynomial* $J_K(N; \exp \frac{2\pi i}{N})$. With this definition, Theorem 1.3 implies (3). Also we obtain the colored Jones polynomial version of Corollary 1.4 of [1] as follows.

Corollary 1.4. *For a hyperbolic knot K with a fixed diagram, assume the assumptions of Proposition 1.1. Let \mathbf{w} be an essential solution of \mathcal{H}_2 , $\mathbf{w}^{(0)}$ be the geometric solution of \mathcal{H}_2 , and $\rho_{\mathbf{w}} : \pi_1(S^3 - K) \rightarrow \mathrm{PSL}(2, \mathbb{C})$ be the parabolic representation induced by \mathbf{w} . Also assume the corresponding solutions \mathbf{z} and $\mathbf{z}^{(0)}$ of \mathcal{H}_1 , determined by \mathbf{w} and $\mathbf{w}^{(0)}$ respectively from Lemma 1.2, are essential. Then*

$$W_0(\mathbf{w}) \equiv i(\mathrm{vol}(\rho_{\mathbf{w}}) + i \mathrm{cs}(\rho_{\mathbf{w}})) \pmod{\pi^2},$$

where $\mathrm{vol}(\rho_{\mathbf{w}}) + i \mathrm{cs}(\rho_{\mathbf{w}})$ is the complex volume of $\rho_{\mathbf{w}}$ defined in [18]. Furthermore, the following inequality holds:

$$\mathrm{Im} W_0(\mathbf{w}) \leq \mathrm{Im} W_0(\mathbf{w}^{(0)}) = \mathrm{vol}(K). \quad (4)$$

The equality of (4) holds if and only if $\mathbf{w} = \mathbf{w}^{(0)}$.

Proof. It is a well-known fact that the hyperbolic volume is the maximal value of volumes of all possible $\mathrm{PSL}(2, \mathbb{C})$ representations and the maximum happens if and only if the representation is discrete and faithful. (For the proof and details, see [3].)

From the proof of Lemma 1.2, if \mathbf{w} and \mathbf{z} are essential, then the shapes of each (collapsed) octahedra in Figure 2 and Figure 10 of Yokota and Thurston triangulations coincide. Therefore, these triangulations form the same geometric shape, and the parabolic representation $\rho_{\mathbf{w}}$ coincides with $\rho_{\mathbf{z}}$ up to conjugate, where $\rho_{\mathbf{w}}$ and $\rho_{\mathbf{z}}$ are the parabolic representations induced by \mathbf{w} and \mathbf{z} respectively. It also implies $\mathbf{z}^{(0)}$ is the geometric solution of \mathcal{H}_1 .

Yokota proved

$$V_0(\mathbf{z}^{(0)}) \equiv i(\mathrm{vol}(K) + i \mathrm{cs}(K)) \pmod{\pi^2},$$

in [17] using Zickert's formula of [18], but the formula also holds for any parabolic representation $\rho_{\mathbf{z}}$ induced by \mathbf{z} . Therefore, Yokota's proof also implies

$$V_0(\mathbf{z}) \equiv i(\mathrm{vol}(\rho_{\mathbf{z}}) + i \mathrm{cs}(\rho_{\mathbf{z}})) \pmod{\pi^2}.$$

Among the essential solutions \mathbf{z} of \mathcal{H}_1 , only the geometric solution $\mathbf{z}^{(0)}$ induces the discrete faithful representation. Therefore, applying Theorem 1.3, we complete the proof. \square

This article consists of the following contents. In Section 2, we describe Yokota triangulation and Thurston triangulation, which correspond to the Kashaev invariant and the colored Jones polynomial respectively. We show that these two triangulations are related by finite

steps of 3-2 moves and 4-5 moves on some crossings. In Section 3, the potential functions V and W are defined. In Section 4, we explain the geometries of V and W , and prove Proposition 1.1. In Section 5, we introduce several dilogarithm identities and then complete the proofs of Lemma 1.2 and Theorem 1.3 using these identities. Finally, in Appendix, we show the potential function W defined in Section 3 can be obtained by the formal substitution of the colored Jones polynomial.

2 Two ideal triangulations of the knot complement

In this section, we explain two ideal triangulations of the knot complement. One is Yokota triangulation corresponding to the Kashaev invariant in [17] and the other is Thurston triangulation corresponding to the colored Jones polynomial in [13]. A good reference of this section is [9], which contains wonderful pictures.

2.1 Yokota triangulation

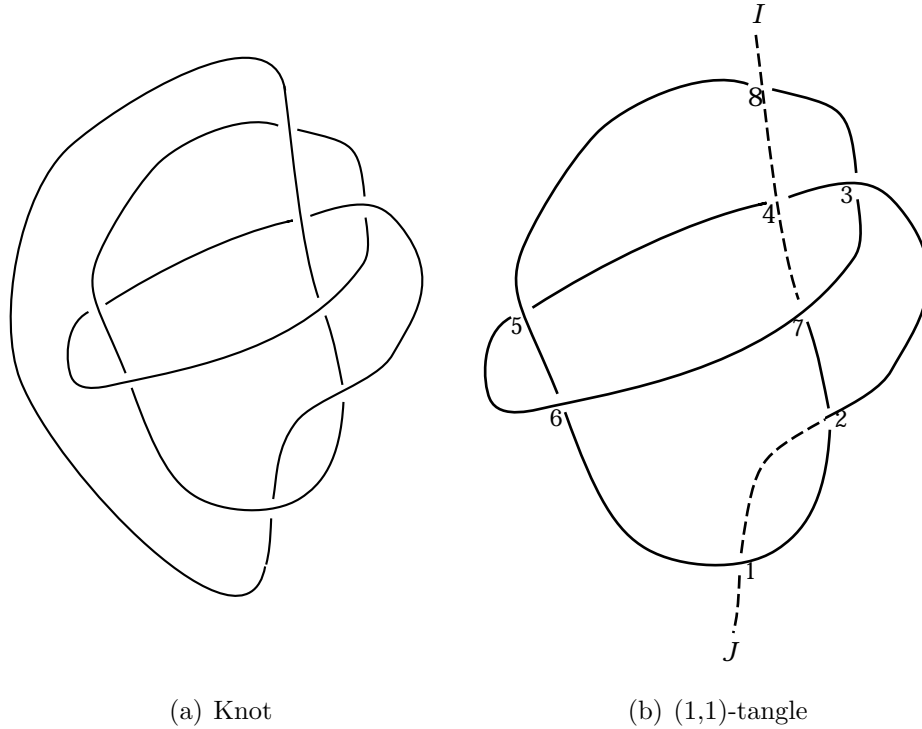


Figure 1: Example

Consider a hyperbolic knot K and its diagram D . (See Figure 1(a).) We define *sides* of D as arcs connecting two adjacent crossing points. For example, Figure 1(a) has 16 sides.

Now split a side of D open so as to make a (1,1)-tangle diagram and label crossings with integers. (See Figure 1(b).) Yokota assumed several conditions on this (1,1)-tangle diagram. (For the exact statement, see **Assumption 1.1–1.4.** and **Assumption 2.2.** in [17].) The assumptions roughly mean that we remove all the crossing points that can be reduced trivially. Also, let the two open sides be I and J and consider the orientation from J to I . Assume I and J are in an over-bridge and in an under-bridge respectively. (Over-bridge is a union of sides, following the orientation of the knot diagram, from one over-crossing point to the next under-crossing point. Under-bridge is the one from one under-crossing point to the next over-crossing point. The boundary endpoints of I and J are considered over-crossing point and under-crossing point respectively. For example, in Figure 1(b), if we follow the diagram from the below to the top, the first under-bridge containing J ends at the crossing 2, and the first over-bridge starts at the crossing 2 and ends at the crossing 4. In total, it has 5 over-bridges and 5 under-bridges. Note that if we change the orientation, the numbers of over-bridges and under-bridges change.)

Now extend I and J so that, when following the orientation of the knot diagram, non-boundary endpoints of I and J become the last under-crossing point and the first over-crossing point respectively, as in Figure 1(b). Then we assume the two non-boundary endpoints of I and J do not coincide, because, if they coincide, then we cut other side open and make a different tangle diagram. Yokota proved in [17] that we can always make two non-boundary endpoints different by cutting certain side open because, if not, then the diagram should be that of a link or the trefoil knot. (For details, see **Assumption 1.3.** and the discussion follows in [17].)

To obtain an ideal triangulation of the knot complement, we place an ideal octahedron $A_n B_n C_n D_n E_n F_n$ on each crossing n as in Figure 2(a). We call the edges $A_n B_n$, $B_n C_n$, $C_n D_n$ and $D_n A_n$ of the octahedron *horizontal edges*. Figure 2(b) shows the positions of A_n , B_n , C_n , D_n and the horizontal edges. We twist the octahedron by identifying edges $A_n E_n$ to $C_n E_n$ and $B_n F_n$ to $D_n F_n$ as in Figure 2(a). (The actual shape of the result was appeared in [9].) Then we glue the faces of the twisted octahedron following the knot diagram. For example, in Figure 2(b), we glue $\triangle A_1 E_1 D_1 \cup \triangle C_1 E_1 D_1$ to $\triangle A_2 F_2 D_2 \cup \triangle A_2 F_2 B_2$, $\triangle C_2 F_2 D_2 \cup \triangle C_2 F_2 B_2$ to $\triangle A_3 F_3 D_3 \cup \triangle A_3 F_3 B_3$, $\triangle C_3 F_3 D_3 \cup \triangle C_3 F_3 B_3$ to $\triangle A_4 E_4 B_4 \cup \triangle C_4 E_4 B_4$, $\triangle A_4 E_4 D_4 \cup \triangle C_4 E_4 D_4$ to $\triangle C_5 E_5 D_5 \cup \triangle A_5 E_5 D_5$, and so on. Finally, we glue $\triangle D_8 F_8 C_8 \cup \triangle B_8 F_8 C_8$ to $\triangle A_1 E_1 B_1 \cup \triangle C_1 E_1 B_1$. Note that, by this gluing, all A_n and C_n are identified to one point, all B_n and D_n are identified to another point, and all E_n and F_n are identified to another point. Let these points be $-\infty$, ∞ and ℓ respectively. Then the regular neighborhoods of $-\infty$ and ∞ become 3-balls, whereas the one of ℓ becomes the tubular neighborhood of the knot K .

We split each octahedron $A_n B_n C_n D_n E_n F_n$ into four tetrahedra, $A_n B_n E_n F_n$, $B_n C_n E_n F_n$, $C_n D_n E_n F_n$ and $D_n A_n E_n F_n$. Then we collapse faces that lies on the split sides. For example, in Figure 2(b), we collapse the faces $\triangle A_1 E_1 B_1 \cup \triangle C_1 E_1 B_1$ and $\triangle D_8 F_8 C_8 \cup \triangle B_8 F_8 C_8$ to different points. Note that this face collapsing makes some edges on these faces into points. Actually the non-horizontal edges $A_2 F_2$, $B_4 F_4$, $D_4 F_4$, $D_7 E_7$, and the horizontal edges $B_2 C_2$, $A_3 B_3$, $A_5 B_5$, $A_6 B_6$ in Figure 2(b) are collapsed to points because of the face collapsing. This makes the tetrahedra $A_1 B_1 E_1 F_1$, $B_1 C_1 E_1 F_1$, $C_1 D_1 E_1 F_1$, $D_1 A_1 E_1 F_1$, $A_2 B_2 E_2 F_2$, $B_2 C_2 E_2 F_2$, $D_2 A_2 E_2 F_2$, $A_3 B_3 E_3 F_3$, $A_4 B_4 E_4 F_4$, $B_4 C_4 E_4 F_4$, $C_4 D_4 E_4 F_4$, $D_4 A_4 E_4 F_4$, $A_5 B_5 E_5 F_5$, $A_6 B_6 E_6 F_6$,

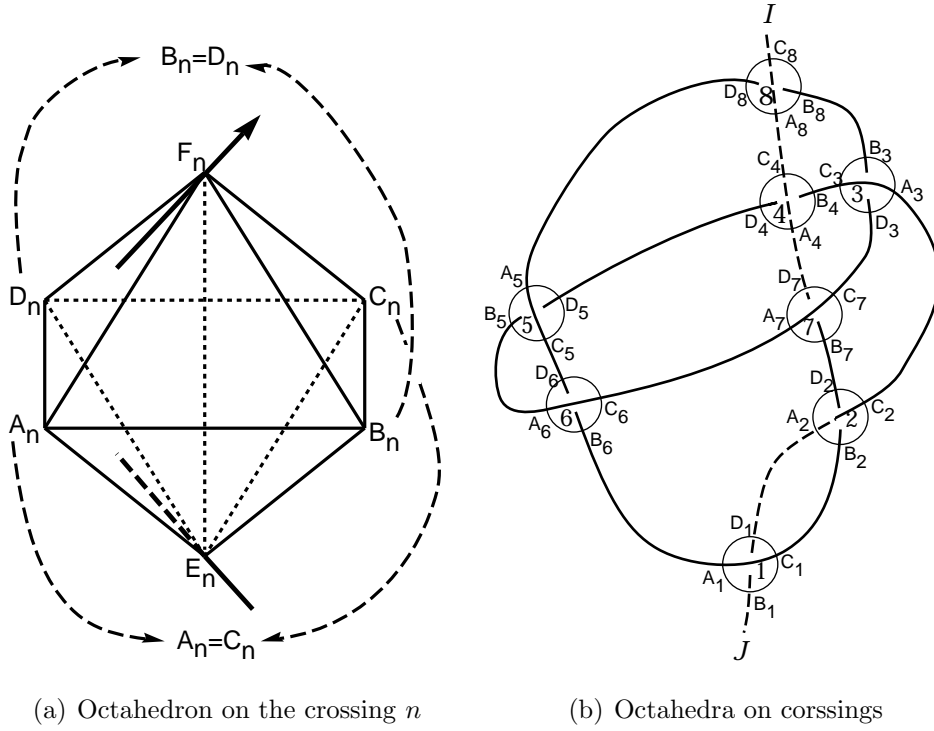


Figure 2: Example(continued)

$C_7D_7E_7F_7$, $D_7A_7E_7F_7$, $A_8B_8E_8F_8$, $B_8C_8E_8F_8$, $C_8D_8E_8F_8$ and $D_8A_8E_8F_8$ be collapsed to points or edges.

The survived tetrahedra after the collapsing can be depicted as follows. At first, remove I and J on the tangle diagram and denote the result G . (See Figure 3.) Note that, by removing $I \cup J$, some vertices are removed, two vertices become trivalent and some sides are glued together. In Figure 3, vertices 1, 4, 8 are removed, 2, 7 become trivalent and G has 9 sides. (We consider the trivalent vertices do not glue any sides.) Now we remove the horizontal edges on the removed vertices, the horizontal edges that is adjacent to $I \cup J$ and the horizontal edges in the unbounded region. (See Figure 3 for the result.) The survived horizontal edges mean the survived ideal tetrahedra after the collapsing. In the example, 12 tetrahedra are survived.

The collapsing identifies the points ∞ , $-\infty$, ℓ each other and connects the regular neighborhoods of them. Collapsing certain edges of a tetrahedron may change the topological type of ℓ , but Yokota excluded such cases by **Assumption 1.1.–1.3.** on the shape of the knot diagram. (**Assumption 1.1.–1.2.** roughly means the diagram has no redundant crossings and **Assumption 1.3.** means the two non-boundary endpoints of I and J do not coincide.) Therefore, the result of the collapsing makes the neighborhood of $\infty = -\infty = \ell$ to be the tubular neighborhood of the knot, and we obtain the ideal triangulation of the knot complement. (See [17] for a complete discussion.)

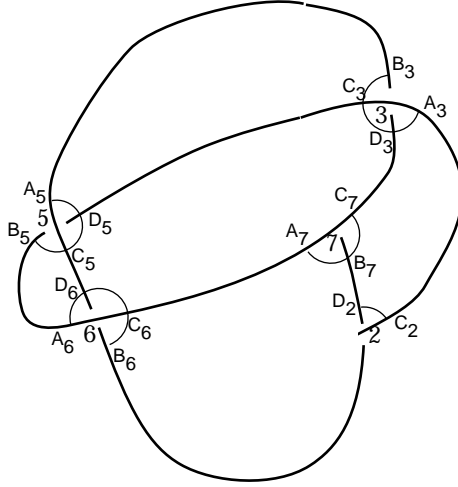


Figure 3: G with survived tetrahedra

2.2 Thurston triangulation

Thurston triangulation, introduced in [13], uses the same octahedra and the same collapsing process, so it also induces an ideal triangulation of the knot complement. However it uses different subdivision of each octahedra. In Figure 2(a), Yokota triangulation subdivides each octahedron into four tetrahedra. However, Thurston triangulation subdivides it into five tetrahedra, $A_n B_n D_n F_n$, $B_n C_n D_n F_n$, $A_n B_n C_n D_n$, $A_n B_n C_n E_n$ and $A_n C_n D_n E_n$. (See the right side of Figure 4(a) for the shape of the subdivision.) In this subdivision, if we apply the collapsing process, some pair of tetrahedra shares the same four vertices. (See the first case of (Case 2) in the proof of Observation 2.1 for an example.) For the convenience of discussion, when this happens, we remove these two tetrahedra and call the result Thurston triangulation.

To see the relation of these two triangulations, we define *4-5 move* of an octahedron and *3-2 move* of a hexahedron as in Figure 4.

Before the collapsing process, two triangulations are related by only 4-5 moves on each crossings. However, the following observation shows they are actually related by 4-5 moves and 3-2 moves on some crossings after the collapsing.

Observation 2.1. *For a hyperbolic knot K with a fixed diagram, if the diagram satisfies **Assumption 1.1.–1.4.** and **Assumption 2.2.** in [17], then Yokota triangulation and Thurston triangulation are related by 3-2 moves and 4-5 moves on some crossings.*

Proof. At first, for a non-trivalent vertex n of G , we show only one horizontal edge in Figure 2(a) can be collapsed. If any of two horizontal edges are collapsed, then the (1,1)-tangle diagram should be Figure 5(a) or Figure 5(b) for some tangle diagrams K_1 and K_2 because the collapsed edges should lie in the unbounded regions. However, Figure 5(a) is excluded because, if we close up the open side, then $K = K_1 \# K_2$ and K cannot be prime. We can

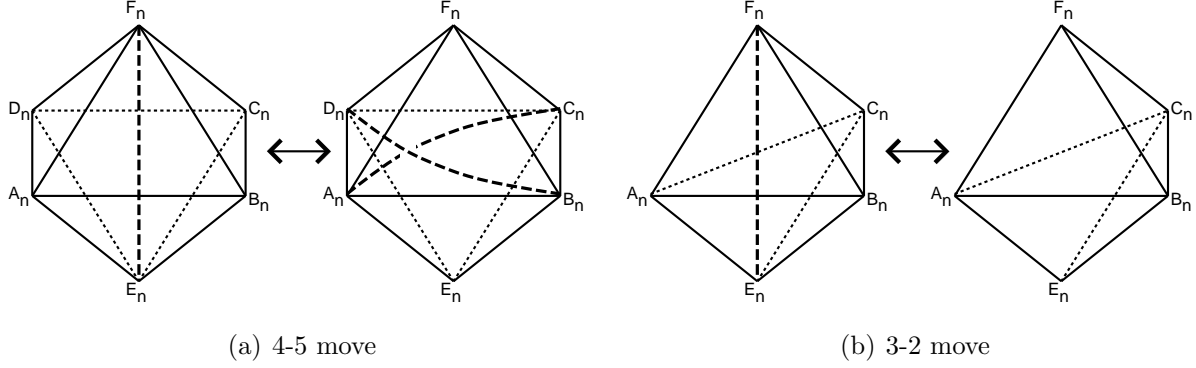


Figure 4: 4-5 and 3-2 moves

also exclude Figure 5(b) because it violates **Assumption 1.1.** in [17]. Actually, in the later case, we can reduce the number of crossings as in Figure 5(b).

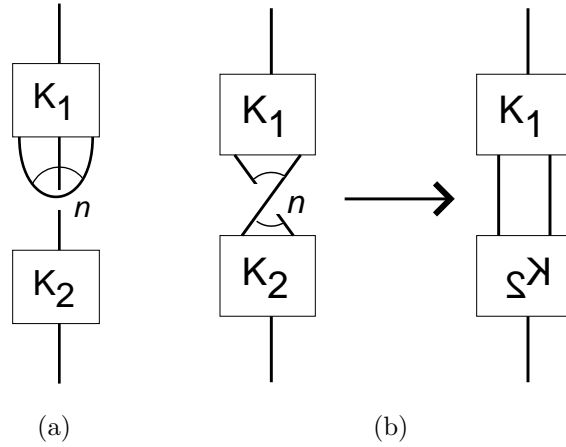


Figure 5: When two horizontal edges are collapsed

Because of this and Yokota's Assumptions, all the cases of collapsing edges in Figure 2(a) are as follows :

(Case 1) if n is a non-trivalent vertex of G , then none or one of the horizontal edges is collapsed.

(Case 2) if n is a trivalent vertex of G , then

1. $D_n E_n$ is collapsed and none or one of $A_n B_n$, $B_n C_n$ is collapsed,
2. $B_n E_n$ is collapsed and none or one of $C_n D_n$, $D_n A_n$ is collapsed,
3. $A_n F_n$ is collapsed and none or one of $B_n C_n$, $C_n D_n$ is collapsed.

It is trivial in (Case 1), so we consider the first case of (Case 2).

If $D_n E_n$ and $A_n B_n$ are collapsed, then the survived tetrahedron is $B_n C_n E_n F_n$ in Yokota triangulation, and $B_n C_n D_n F_n$ in Thurston triangulation. They coincide because $D_n = E_n$ by the collapsing of $D_n E_n$.

If $D_n E_n$ is collapsed and no others, then the survived tetrahedra are $A_n B_n E_n F_n$ and $B_n C_n E_n F_n$ in Yokota triangulation, and $A_n B_n D_n F_n$, $B_n C_n D_n F_n$, $A_n B_n C_n D_n$ and $A_n B_n C_n E_n$ in Thurston triangulation. However, in Thurston triangulation, two tetrahedra $A_n B_n C_n D_n$ and $A_n B_n C_n E_n$ are canceled each other because they share the same vertices A_n, B_n, C_n and $D_n = E_n$. The others coincide with the tetrahedra in Yokota triangulation because $D_n = E_n$.

Other cases of (Case 2) is the same with the first case, so the proof is completed. \square

3 Potential functions

3.1 The case of Kashaev invariant

In the case of Kashaev invariant, Yokota's potential function $V(z_1, \dots, z_g)$ is defined by the following way.

For the graph G , we define *contributing sides* as sides of G which are not on the unbounded regions. For example, there are 5 contributing sides and 4 non-contributing sides in Figure 6. We assign complex variables z_1, \dots, z_g to contributing sides and real number 1 to non-contributing sides. Then we label each ideal tetrahedra with IT_1, IT_2, \dots, IT_s and assign t_l ($l = 1, \dots, s$) to the horizontal edge of IT_l as the shape parameter. We define t_l as the counterclockwise ratio of the complex variables z_1, \dots, z_g .

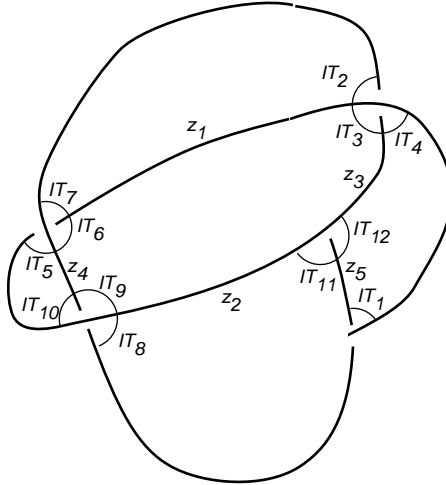


Figure 6: G with contributing sides

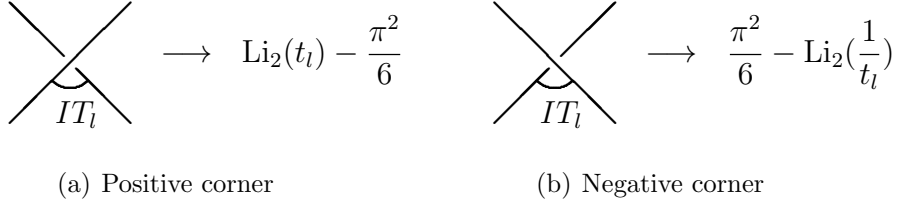


Figure 7: Assigning dilogarithm functions to each tetrahedra

For example, in Figure 6,

$$t_1 = \frac{z_5}{1}, t_2 = \frac{z_1}{1}, t_3 = \frac{z_3}{z_1}, t_4 = \frac{1}{z_3}, t_5 = \frac{z_4}{1}, t_6 = \frac{z_1}{z_4},$$

$$t_7 = \frac{1}{z_1}, t_8 = \frac{z_2}{1}, t_9 = \frac{z_4}{z_2}, t_{10} = \frac{1}{z_4}, t_{11} = \frac{z_5}{z_2}, t_{12} = \frac{z_3}{z_5}.$$

For each tetrahedron IT_l , we assign dilogarithm function as in Figure 7. Then we define $V(z_1, \dots, z_g)$ by the summation of all these dilogarithm functions. We also define the sign σ_l of IT_l by

$$\sigma_l = \begin{cases} 1 & \text{if } IT_l \text{ lies as in Figure 7(a),} \\ -1 & \text{if } IT_l \text{ lies as in Figure 7(b).} \end{cases}$$

Then $V(z_1, \dots, z_g)$ is expressed by

$$V(z_1, \dots, z_g) = \sum_{l=1}^g \sigma_l \left(\text{Li}_2(t_l^{\sigma_l}) - \frac{\pi^2}{6} \right).$$

For example, in Figure 6,

$$\sigma_1 = \sigma_3 = \sigma_6 = \sigma_9 = \sigma_{11} = 1, \sigma_2 = \sigma_4 = \sigma_5 = \sigma_7 = \sigma_8 = \sigma_{10} = \sigma_{12} = -1,$$

and

$$V(z_1, \dots, z_5) = \text{Li}_2(z_5) - \text{Li}_2\left(\frac{1}{z_1}\right) + \text{Li}_2\left(\frac{z_3}{z_1}\right) - \text{Li}_2(z_3) - \text{Li}_2\left(\frac{1}{z_4}\right) + \text{Li}_2\left(\frac{z_1}{z_4}\right)$$

$$- \text{Li}_2(z_1) - \text{Li}_2\left(\frac{1}{z_2}\right) + \text{Li}_2\left(\frac{z_4}{z_2}\right) - \text{Li}_2(z_4) + \text{Li}_2\left(\frac{z_5}{z_2}\right) - \text{Li}_2\left(\frac{z_5}{z_3}\right) + \frac{\pi^2}{3}.$$

It was shown in [16] that $V(z_1, \dots, z_g)$ can be obtained by the formal substitution of the Kashaev invariant.¹

3.2 The case of colored Jones polynomial

For each region of G , we choose one bounded region and assign 1 to it. Then we assign variables w_1, \dots, w_m to the other bounded regions, and 0 to the unbounded region. (See Figure 8.)

¹ We remark that the Kashaev invariant of a knot K defined in [16] is the one of the mirror image \overline{K} defined in [10]. This article follows the definition of [16].

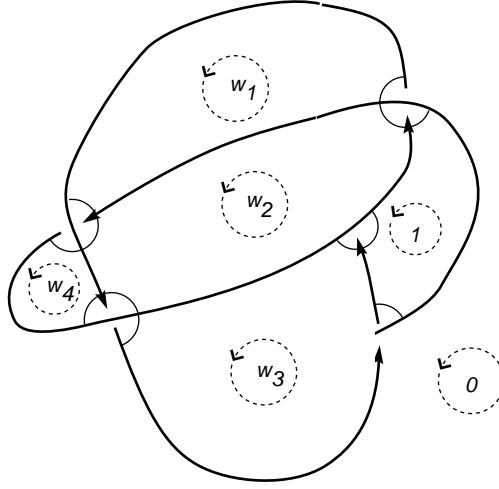


Figure 8: Assigning variables on each regions

For each vertices of G , we assign the following functions according to the type of the vertex and the horizontal edges : For positive crossings :

$$\begin{aligned}
 & \begin{array}{c} \text{Diagram 1: } w_l \text{ and } w_m \text{ cross } w_k \text{ and } w_j \text{ with } w_l \text{ and } w_m \text{ on the left and } w_k \text{ and } w_j \text{ on the right.} \\ \text{Diagram 2: } w_l \text{ and } w_m \text{ cross } w_k \text{ and } w_j \text{ with } w_l \text{ and } w_m \text{ on the left and } w_k \text{ and } w_j \text{ on the right.} \\ \text{Diagram 3: } w_l \text{ and } w_m \text{ cross } w_k \text{ and } w_j \text{ with } w_l \text{ and } w_m \text{ on the left and } w_k \text{ and } w_j \text{ on the right.} \\ \text{Diagram 4: } w_l \text{ and } w_m \text{ cross } w_k \text{ and } w_j \text{ with } w_l \text{ and } w_m \text{ on the left and } w_k \text{ and } w_j \text{ on the right.} \end{array} \\
 & : P_1(w_j, w_k, w_l, w_m) = -\text{Li}_2\left(\frac{w_l}{w_m}\right) - \text{Li}_2\left(\frac{w_l}{w_k}\right) + \text{Li}_2\left(\frac{w_j w_l}{w_k w_m}\right) \\
 & \quad + \text{Li}_2\left(\frac{w_m}{w_j}\right) + \text{Li}_2\left(\frac{w_k}{w_j}\right) - \frac{\pi^2}{6} + \log \frac{w_m}{w_j} \log \frac{w_k}{w_j}, \\
 & : P_2(w_j, w_k, w_l, w_m) = \text{Li}_2\left(\frac{w_m}{w_l}\right) - \text{Li}_2\left(\frac{w_l}{w_k}\right) - \text{Li}_2\left(\frac{w_k w_m}{w_j w_l}\right) \\
 & \quad + \text{Li}_2\left(\frac{w_m}{w_j}\right) - \text{Li}_2\left(\frac{w_j}{w_k}\right) + \frac{\pi^2}{6} - \log \frac{w_k}{w_l} \log \frac{w_k}{w_j}, \\
 & : P_3(w_j, w_k, w_l, w_m) = \text{Li}_2\left(\frac{w_m}{w_l}\right) + \text{Li}_2\left(\frac{w_k}{w_l}\right) + \text{Li}_2\left(\frac{w_j w_l}{w_k w_m}\right) \\
 & \quad - \text{Li}_2\left(\frac{w_j}{w_m}\right) - \text{Li}_2\left(\frac{w_j}{w_k}\right) - \frac{\pi^2}{6} + \log \frac{w_m}{w_l} \log \frac{w_k}{w_l}, \\
 & : P_4(w_j, w_k, w_l, w_m) = -\text{Li}_2\left(\frac{w_l}{w_m}\right) + \text{Li}_2\left(\frac{w_k}{w_l}\right) - \text{Li}_2\left(\frac{w_k w_m}{w_j w_l}\right) \\
 & \quad - \text{Li}_2\left(\frac{w_j}{w_m}\right) + \text{Li}_2\left(\frac{w_k}{w_j}\right) + \frac{\pi^2}{6} - \log \frac{w_m}{w_l} \log \frac{w_m}{w_j}.
 \end{aligned}$$

For negative crossings :

$$\begin{aligned}
 & \begin{array}{c} \text{Diagram 1: } w_l \text{ and } w_m \text{ cross } w_k \text{ and } w_j \text{ with } w_l \text{ and } w_m \text{ on the left and } w_k \text{ and } w_j \text{ on the right.} \\ \text{Diagram 2: } w_l \text{ and } w_m \text{ cross } w_k \text{ and } w_j \text{ with } w_l \text{ and } w_m \text{ on the left and } w_k \text{ and } w_j \text{ on the right.} \end{array} \\
 & : N_1(w_j, w_k, w_l, w_m) = \text{Li}_2\left(\frac{w_l}{w_m}\right) + \text{Li}_2\left(\frac{w_l}{w_k}\right) - \text{Li}_2\left(\frac{w_j w_l}{w_k w_m}\right) \\
 & \quad - \text{Li}_2\left(\frac{w_m}{w_j}\right) - \text{Li}_2\left(\frac{w_k}{w_j}\right) + \frac{\pi^2}{6} - \log \frac{w_j}{w_m} \log \frac{w_j}{w_k}, \\
 & : N_2(w_j, w_k, w_l, w_m) = -\text{Li}_2\left(\frac{w_m}{w_l}\right) + \text{Li}_2\left(\frac{w_l}{w_k}\right) + \text{Li}_2\left(\frac{w_k w_m}{w_j w_l}\right) \\
 & \quad - \text{Li}_2\left(\frac{w_m}{w_j}\right) + \text{Li}_2\left(\frac{w_j}{w_k}\right) - \frac{\pi^2}{6} + \log \frac{w_l}{w_k} \log \frac{w_j}{w_k},
 \end{aligned}$$

$$\begin{array}{l}
\begin{array}{c} \nearrow w_l \\ \circlearrowleft \\ \nwarrow w_m \end{array} \begin{array}{c} \nearrow w_k \\ \circlearrowright \\ \nwarrow w_j \end{array} : N_3(w_j, w_k, w_l, w_m) = -\text{Li}_2\left(\frac{w_m}{w_l}\right) - \text{Li}_2\left(\frac{w_k}{w_l}\right) - \text{Li}_2\left(\frac{w_j w_l}{w_k w_m}\right) \\
\hspace{15em} + \text{Li}_2\left(\frac{w_j}{w_m}\right) + \text{Li}_2\left(\frac{w_j}{w_k}\right) + \frac{\pi^2}{6} - \log \frac{w_l}{w_m} \log \frac{w_l}{w_k}, \\
\begin{array}{c} \nearrow w_l \\ \circlearrowright \\ \nwarrow w_m \end{array} \begin{array}{c} \nearrow w_k \\ \circlearrowleft \\ \nwarrow w_j \end{array} : N_4(w_j, w_k, w_l, w_m) = \text{Li}_2\left(\frac{w_l}{w_m}\right) - \text{Li}_2\left(\frac{w_k}{w_l}\right) + \text{Li}_2\left(\frac{w_k w_m}{w_j w_l}\right) \\
\hspace{15em} + \text{Li}_2\left(\frac{w_j}{w_m}\right) - \text{Li}_2\left(\frac{w_k}{w_j}\right) - \frac{\pi^2}{6} + \log \frac{w_l}{w_m} \log \frac{w_j}{w_m}.
\end{array}$$

If no horizontal edge is collapsed at the positive or negative crossing, we assign any of P_1, \dots, P_4 or N_1, \dots, N_4 to the crossing respectively. In Lemma 3.1, we will show this choice does not have any effect on the optimistic limit of the colored Jones polynomial.

For the end points of I and J , we use the same formula whether certain horizontal edge is collapsed or not. For the end point of I :

$$\begin{array}{l}
\begin{array}{c} \nearrow w_l \\ \circlearrowleft \\ \nwarrow w_m \end{array} \begin{array}{c} \nearrow w_k \\ \circlearrowright \\ \nwarrow w_j \end{array} : P_1(w_j, w_j, w_l, w_m) = P_2(w_j, w_j, w_l, w_m) = \text{Li}_2\left(\frac{w_m}{w_j}\right) - \text{Li}_2\left(\frac{w_l}{w_j}\right), \\
\begin{array}{c} \nearrow w_l \\ \circlearrowright \\ \nwarrow w_m \end{array} \begin{array}{c} \nearrow w_k \\ \circlearrowleft \\ \nwarrow w_j \end{array} : N_1(w_j, w_k, w_l, w_j) = N_4(w_j, w_k, w_l, w_j) = -\text{Li}_2\left(\frac{w_k}{w_j}\right) + \text{Li}_2\left(\frac{w_l}{w_j}\right).
\end{array}$$

For the end point of J :

$$\begin{array}{l}
\begin{array}{c} \nearrow w_l \\ \circlearrowleft \\ \nwarrow w_m \end{array} \begin{array}{c} \nearrow w_k \\ \circlearrowright \\ \nwarrow w_j \end{array} : P_2(w_j, w_k, w_k, w_m) = P_3(w_j, w_k, w_k, w_m) = \text{Li}_2\left(\frac{w_m}{w_k}\right) - \text{Li}_2\left(\frac{w_j}{w_k}\right), \\
\begin{array}{c} \nearrow w_l \\ \circlearrowright \\ \nwarrow w_m \end{array} \begin{array}{c} \nearrow w_k \\ \circlearrowleft \\ \nwarrow w_j \end{array} : N_3(w_j, w_k, w_l, w_l) = N_4(w_j, w_k, w_l, w_l) = -\text{Li}_2\left(\frac{w_k}{w_l}\right) + \text{Li}_2\left(\frac{w_j}{w_l}\right).
\end{array}$$

In Appendix, we show that the assigned functions above are, in fact, obtained by the formal substitution of certain forms of the R-matrix of the colored Jones polynomial.

Now we define the potential function $W(w_1, \dots, w_m)$ of the knot diagram by the summation of all functions assigned to the vertices of G . For an example, the potential function $W(w_1, \dots, w_4)$ of Figure 8 is

$$\begin{aligned}
W(w_1, \dots, w_4) = & -\text{Li}_2\left(\frac{1}{w_3}\right) + \left\{ \text{Li}_2\left(\frac{1}{w_2}\right) + \text{Li}_2\left(\frac{w_1}{w_2}\right) - \frac{\pi^2}{6} + \log \frac{1}{w_2} \log \frac{w_1}{w_2} \right\} \\
& + \left\{ \text{Li}_2\left(\frac{w_1}{w_2}\right) + \text{Li}_2\left(\frac{w_4}{w_2}\right) - \frac{\pi^2}{6} + \log \frac{w_1}{w_2} \log \frac{w_4}{w_2} \right\} \\
& + \left\{ \text{Li}_2\left(\frac{w_4}{w_2}\right) + \text{Li}_2\left(\frac{w_3}{w_2}\right) - \frac{\pi^2}{6} + \log \frac{w_4}{w_2} \log \frac{w_3}{w_2} \right\} + \left\{ \text{Li}_2\left(\frac{1}{w_2}\right) - \text{Li}_2\left(\frac{w_3}{w_2}\right) \right\}.
\end{aligned} \tag{5}$$

We close up this section with the invariance of the optimistic limit under the choice of the four different forms of the potential functions of a crossing.

Lemma 3.1. *For the functions $P_1, \dots, P_4, N_1, \dots, N_4$ defined above, let*

$$P_{f0} := P_f - \sum_{a=j,k,l,m} \left(w_a \frac{\partial P_f}{\partial w_a} \right) \log w_a, \quad N_{f0} := N_f - \sum_{a=j,k,l,m} \left(w_a \frac{\partial N_f}{\partial w_a} \right) \log w_a.$$

Then

$$P_{10} \equiv P_{20} \equiv P_{30} \equiv P_{40}, \quad N_{10} \equiv N_{20} \equiv N_{30} \equiv N_{40} \pmod{4\pi^2},$$

and, for $a = j, k, l, m$,

$$\begin{aligned} \exp \left(w_a \frac{\partial P_1}{\partial w_a} \right) &= \exp \left(w_a \frac{\partial P_2}{\partial w_a} \right) = \exp \left(w_a \frac{\partial P_3}{\partial w_a} \right) = \exp \left(w_a \frac{\partial P_4}{\partial w_a} \right), \\ \exp \left(w_a \frac{\partial N_1}{\partial w_a} \right) &= \exp \left(w_a \frac{\partial N_2}{\partial w_a} \right) = \exp \left(w_a \frac{\partial N_3}{\partial w_a} \right) = \exp \left(w_a \frac{\partial N_4}{\partial w_a} \right). \end{aligned}$$

Proof. For a given complex valued function $F(w_j, w_k, w_l, w_m)$, let

$$\widehat{F}(w_j, w_k, w_l, w_m) := F + \sum_{a=j,k,l,m} 2n_a \pi i \log w_a + 4n\pi^2, \quad (6)$$

for some integer constants n_j, n_k, n_l, n_m, n . Then, by the direct calculation,

$$\widehat{F}_0 \equiv F_0 \pmod{4\pi^2},$$

and

$$\exp \left(w_a \frac{\partial F}{\partial w_a} \right) = \exp \left(w_a \frac{\partial \widehat{F}}{\partial w_a} \right).$$

These show F and \widehat{F} define the same optimistic limit, so we define an equivalence relation \approx by $F \approx \widehat{F}$ for F and \widehat{F} satisfying (6).

For

$$\begin{aligned} P_1 &= -\text{Li}_2\left(\frac{w_l}{w_m}\right) - \text{Li}_2\left(\frac{w_l}{w_k}\right) + \text{Li}_2\left(\frac{w_j w_l}{w_k w_m}\right) + \text{Li}_2\left(\frac{w_m}{w_j}\right) + \text{Li}_2\left(\frac{w_k}{w_j}\right) - \frac{\pi^2}{6} + \log \frac{w_m}{w_j} \log \frac{w_k}{w_j}, \\ P_2 &= \text{Li}_2\left(\frac{w_m}{w_l}\right) - \text{Li}_2\left(\frac{w_l}{w_k}\right) - \text{Li}_2\left(\frac{w_k w_m}{w_j w_l}\right) + \text{Li}_2\left(\frac{w_m}{w_j}\right) - \text{Li}_2\left(\frac{w_j}{w_k}\right) + \frac{\pi^2}{6} - \log \frac{w_k}{w_l} \log \frac{w_k}{w_j}, \end{aligned}$$

using the well-known identity $\text{Li}_2(z) + \text{Li}_2(\frac{1}{z}) \approx -\frac{\pi^2}{6} - \frac{1}{2} \log^2(-z)$ for $z \in \mathbb{C}$ in [5], we obtain

$$\begin{aligned} P_1 - P_2 &= -\text{Li}_2\left(\frac{w_l}{w_m}\right) - \text{Li}_2\left(\frac{w_m}{w_l}\right) + \text{Li}_2\left(\frac{w_j w_l}{w_k w_m}\right) + \text{Li}_2\left(\frac{w_k w_m}{w_j w_l}\right) \\ &\quad + \text{Li}_2\left(\frac{w_k}{w_j}\right) + \text{Li}_2\left(\frac{w_j}{w_k}\right) - \frac{\pi^2}{3} + \left(\log \frac{w_m}{w_j} + \log \frac{w_k}{w_l} \right) \log \frac{w_k}{w_j} \\ &\approx -\frac{\pi^2}{2} + \frac{1}{2} \log^2\left(-\frac{w_l}{w_m}\right) - \frac{1}{2} \log^2\left(-\frac{w_k w_m}{w_j w_l}\right) - \frac{1}{2} \log^2\left(-\frac{w_k}{w_j}\right) + \left(\log \frac{w_m}{w_j} + \log \frac{w_k}{w_l} \right) \log \frac{w_k}{w_j}. \end{aligned}$$

Remark that, for any integer n , some integers n_1, \dots, n_4 and indices $a, b \in \{i, j, k, l\}$, we have

$$\begin{aligned}
2n\pi i \log \frac{w_a}{w_b} &= 2n\pi i (\log w_a - \log w_b + 2n_1\pi i) \approx 0, \\
\frac{1}{2} \log^2\left(-\frac{w_k}{w_j}\right) &= \frac{1}{2} \left\{ \log \frac{w_k}{w_j} + (2n_2 - 1)\pi i \right\}^2 \\
&= \frac{1}{2} \log^2 \frac{w_k}{w_j} + (2n_2 - 1)\pi i \log \frac{w_k}{w_j} - 2n_2(n_2 - 1)\pi^2 - \frac{\pi^2}{2} \\
&\approx \frac{1}{2} \log^2 \frac{w_k}{w_j} - \pi i \log \frac{w_k}{w_j} - \frac{\pi^2}{2},
\end{aligned}$$

and

$$\begin{aligned}
\frac{1}{2} \left\{ \log \frac{w_k}{w_j} - \log\left(-\frac{w_k w_m}{w_j w_l}\right) \right\}^2 &= \frac{1}{2} \left\{ \log\left(-\frac{w_l}{w_m}\right) + 2n_3\pi i \right\}^2 \\
&= \frac{1}{2} \log^2\left(-\frac{w_l}{w_m}\right) + 2n_3\pi i \left\{ \log \frac{w_l}{w_m} + (2n_4 + 1)\pi i \right\} - 2n_3^2\pi^2 \\
&\approx \frac{1}{2} \log^2\left(-\frac{w_l}{w_m}\right) - 2n_3(n_3 + 1)\pi^2 \approx \frac{1}{2} \log^2\left(-\frac{w_l}{w_m}\right).
\end{aligned}$$

Therefore, we obtain

$$\begin{aligned}
P_1 - P_2 &\approx \frac{1}{2} \log^2\left(-\frac{w_l}{w_m}\right) - \frac{1}{2} \log^2\left(-\frac{w_k w_m}{w_j w_l}\right) - \frac{1}{2} \log^2 \frac{w_k}{w_j} + \pi i \log \frac{w_k}{w_j} + \log \frac{w_k w_m}{w_j w_l} \log \frac{w_k}{w_j} \\
&\approx \frac{1}{2} \log^2\left(-\frac{w_l}{w_m}\right) - \frac{1}{2} \log^2\left(-\frac{w_k w_m}{w_j w_l}\right) - \frac{1}{2} \log^2 \frac{w_k}{w_j} + \log\left(-\frac{w_k w_m}{w_j w_l}\right) \log \frac{w_k}{w_j} \\
&= \frac{1}{2} \log^2\left(-\frac{w_l}{w_m}\right) - \frac{1}{2} \left\{ \log \frac{w_k}{w_j} - \log\left(-\frac{w_k w_m}{w_j w_l}\right) \right\}^2 \approx \frac{1}{2} \log^2\left(-\frac{w_l}{w_m}\right) - \frac{1}{2} \log^2\left(-\frac{w_l}{w_m}\right) = 0.
\end{aligned}$$

Other equalities $P_2 \approx P_3 \approx P_4$ and $N_1 \approx N_2 \approx N_3 \approx N_4$ can be obtained by the same method or by the symmetry of the equations. \square

4 Geometric structures of the triangulations

For Yokota triangulation and Thurston triangulation, we assign complex variables on each tetrahedra and solve certain equations. Then one of the solutions gives the complete hyperbolic structure of the knot complement. We describe these procedures in this section.

At first, consider the following positive and negative crossings in Figure 9, where z_a, z_b, z_c, z_d are the variables assigned to the sides of G and w_j, w_k, w_l, w_m are the variables assigned to the regions of G . Note that z_a, z_b, z_c, z_d and w_j, w_k, w_l, w_m are used for defining the potential functions $V(z_1, \dots, z_g)$ and $W(w_1, \dots, w_m)$ respectively.

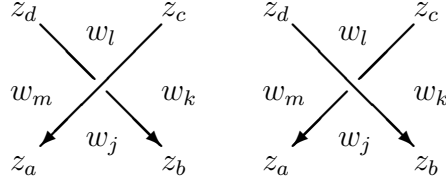


Figure 9: Assignment of variables

Then we consider Figure 10. We assign $\frac{z_b}{z_a}, \frac{z_c}{z_b}, \frac{z_d}{z_c}, \frac{z_a}{z_d}$ to the horizontal edges $C_nD_n, D_nA_n, A_nB_n, B_nC_n$ respectively. This assignment determines the shape parameters of the tetrahedra of Yokota triangulation. Also, for the positive crossing, we assign $\left(\frac{w_j}{w_m}\right)^{-1}, \frac{w_k}{w_j}, \frac{w_k}{w_l}, \left(\frac{w_l}{w_m}\right)^{-1}$ to $C_nF_n, D_nE_n, A_nF_n, B_nE_n$ respectively, and assign $\left(\frac{w_k w_m}{w_j w_l}\right)^{-1}$ to B_nD_n and A_nC_n for the parameter of the tetrahedron $A_nB_nC_nD_n$. For the negative crossing, we assign $\frac{w_j}{w_m}, \left(\frac{w_k}{w_j}\right)^{-1}, \left(\frac{w_k}{w_l}\right)^{-1}, \frac{w_l}{w_m}$ to $B_nE_n, C_nF_n, D_nE_n, A_nF_n$ respectively, and assign $\left(\frac{w_j w_l}{w_k w_m}\right)^{-1}$ to B_nD_n and A_nC_n for the parameter of the tetrahedron $A_nB_nC_nD_n$. These assignments determine the shape parameters of the tetrahedra of Thurston triangulation.

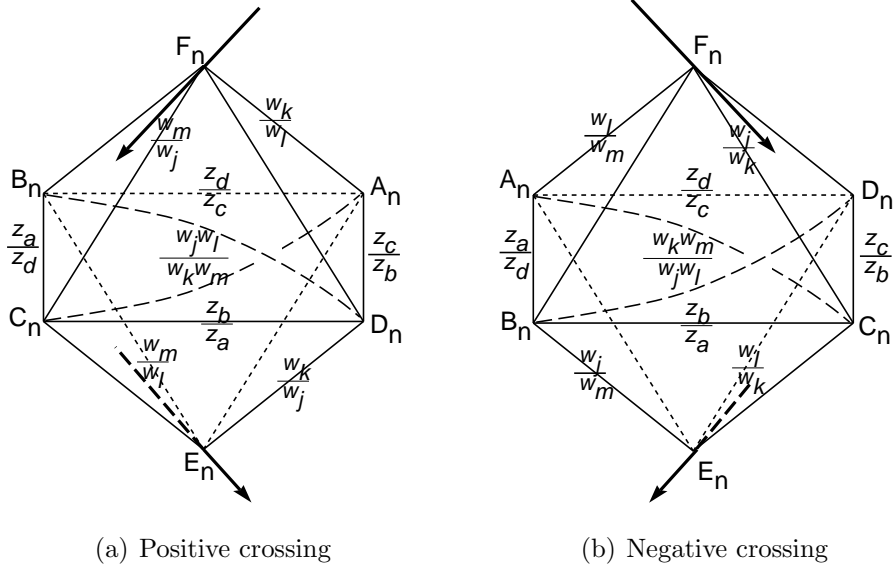


Figure 10: Assignment of shape parameters

We do not assign any shape parameters to the collapsed edges. Also, in the case of Thurston triangulation, we do not assign any shape parameters to the edges that contain the endpoints of the collapsed edges. For example, if C_nD_n is collapsed, then we do not assign any shape parameters to C_nF_n, D_nE_n and B_nD_n . Also, if D_nE_n is collapsed in Figure 10(a), then we do not assign any shape parameters to B_nD_n, B_nE_n, C_nD_n and D_nA_n .²

² The edges C_nD_n and D_nA_n are horizontal edges, but are identified to non-horizontal edges. When this

Yokota and Thurston triangulations are ideal triangulations, so by assigning shape parameters, we can determine all the shapes of the hyperbolic ideal tetrahedra of the triangulations. Note that if we assign a shape parameter $u \in \mathbb{C} - \{0, 1\}$ to an edge of an ideal tetrahedron, then the other edges are also parametrized by $u, u' := \frac{1}{1-u}$ and $u'' := 1 - \frac{1}{u}$ as in Figure 11.

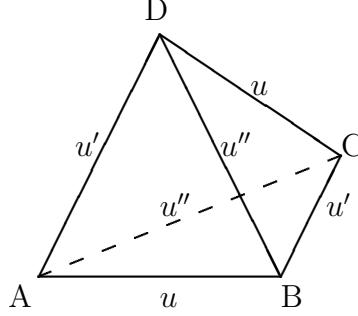


Figure 11: Parametrization of a hyperbolic ideal tetrahedron with shape parameter u

So as to get the hyperbolic structure, these shape parameters should satisfy the *edges relations* and the *cusp conditions*. The edge relations mean the product of all shape parameters assigned to each edge should be 1, and the cusp conditions mean the holonomies induced by the longitude and the meridian should be translations on the cusp. These two conditions can be expressed by set of equations of the shape parameters, so we call the set of equations *hyperbolicity equations*. (For details, see Chapter 4 of [14].) We call a solution (z_1, \dots, z_g) of the hyperbolicity equations of Yokota triangulation *essential* if none of the shape parameters of the tetrahedra are one of $0, 1, \infty$. We also define an *essential solution* (w_1, \dots, w_m) of Thurston triangulation in the same way. It is a well-known fact that if the hyperbolicity equations have an essential solution, then they have the unique solution which gives the hyperbolic structure to the triangulation.³ (For details, see Section 2.8 of [15].) We call the unique solution *geometric solution*, and denote the geometric solution of Yokota triangulation $\mathbf{z}^{(0)} = (z_1^{(0)}, \dots, z_g^{(0)})$ and that of Thurston triangulation $\mathbf{w}^{(0)} = (w_1^{(0)}, \dots, w_m^{(0)})$. We remark that, in Theorem 1.3, we assumed the existence of the geometric solutions $\mathbf{z}^{(0)}$ and $\mathbf{w}^{(0)}$.

Yokota proved in [17] that, for the potential function V defined in Section 3.1, $\mathcal{H}_1 = \left\{ \exp \left(z_k \frac{\partial V}{\partial z_k} \right) = 1 \mid k = 1, \dots, g \right\}$ becomes the hyperbolicity equations of Yokota triangulation. In other words, each element of \mathcal{H}_1 becomes an edge relation or a cusp condition for all $k = 1, \dots, g$, and all the other equations are trivially or induced from the elements of \mathcal{H}_1 .

Proposition 1.1 shows the same holds for the potential function W defined in Section 3.2 and $\mathcal{H}_2 = \left\{ \exp \left(w_l \frac{\partial W}{\partial w_l} \right) = 1 \mid l = 1, \dots, m \right\}$. We prove it in this section.

happens, we do not assign shape parameters to these edges.

³ Strictly speaking, we have the unique values of shape parameters. However, these values uniquely determine the solutions $(z_1^{(0)}, \dots, z_g^{(0)})$ and $(w_1^{(0)}, \dots, w_m^{(0)})$. It was explained in [17] for Yokota triangulation, and it will be in the end of this Section for Thurston triangulation.

Let \mathcal{A} be the set of non-collapsed horizontal edges of Thurston triangulation of $S^3 - K$. Let \mathcal{B} be the set of non-collapsed non-horizontal edges $A_n E_n, B_n E_n, C_n E_n, D_n E_n, A_n F_n, B_n F_n, C_n F_n, D_n F_n$ in Figure 10, which are not in \mathcal{A} .⁴ Finally, let \mathcal{C} be the set of edges $A_n C_n, B_n D_n$ in Figure 10, which are not in $\mathcal{A} \cup \mathcal{B}$.

For example, in Figure 3, $\mathcal{A} = \{ A_7 B_7 = B_6 C_6 = D_2 A_2 = D_2 F_2 = A_2 B_2 = B_2 F_2 = C_2 F_2 = A_3 F_3 = B_3 F_3 = D_3 F_3 = D_5 E_5, D_6 A_6 = B_5 C_5, C_6 D_6 = C_5 D_5 = C_3 D_3 = D_7 A_7 = A_7 E_7 = C_7 D_7 = C_7 E_7 = A_2 E_2 = C_2 E_2 = B_2 E_2 = A_6 E_6 = B_6 E_6 = C_6 E_6 = C_5 F_5, D_5 A_5 = B_3 C_3, C_2 D_2 = B_7 C_7 = D_3 A_3 \}$, $\mathcal{B} = \{ D_3 E_3 = B_7 F_7 = D_7 F_7 = A_6 F_6 = B_6 F_6 = D_6 F_6 = B_5 E_5 = C_5 E_5 = A_5 E_5 = C_3 F_3, A_7 F_7 = C_6 F_6, D_6 E_6 = B_5 F_5 = D_5 F_5 = A_5 F_5 = A_3 E_3 = B_3 E_3 = C_3 E_3 = C_7 F_7, B_7 E_7 = D_2 E_2 \}$ and $\mathcal{C} = \emptyset$.

Lemma 4.1. *For a hyperbolic knot K with a fixed diagram, we assume the assumptions of Proposition 1.1. Then the edges in $\mathcal{B} \cup \mathcal{C}$ satisfy the edge relations trivially by the assigning rule of the shape parameters.*

Proof. If an edge $A_n C_n$ or $B_n D_n$ of Figure 10 is in \mathcal{C} , then the octahedron $A_n B_n C_n D_n E_n F_n$ does not have any collapsed edge. By the assigning rule of the shape parameters, all the edges in \mathcal{C} satisfy edge relations trivially.

Now we show the case of \mathcal{B} . Consider the following four cases of two points n_1 and n_2 in Figure 12 and the two regions between the crossings are parametrized by the variables w_a and w_b . (For the positions of the points $A_{n_1}, B_{n_1}, \dots, F_{n_2}$, see Figure 2.) At first, we assume no edges are collapsed in the tetrahedra $A_{n_1} B_{n_1} D_{n_1} F_{n_1}$ and $C_{n_2} B_{n_2} D_{n_2} F_{n_2}$. This means the two regions with w_a and w_b in Figure 12 are bounded.

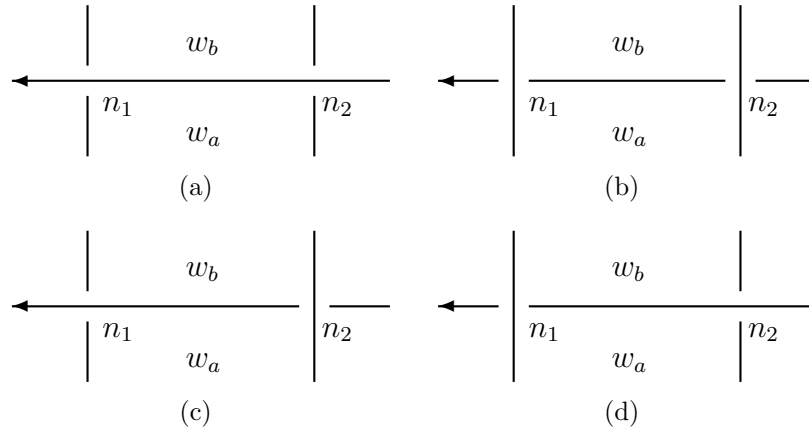


Figure 12: Four cases

In the case of Figure 12(a), we want to prove the edge relation of the edge $A_{n_1} F_{n_1} = C_{n_2} F_{n_2} \in \mathcal{B}$ holds trivially. We draw a part of the cusp diagram in $A_{n_1} B_{n_1} D_{n_1} F_{n_1} \cup C_{n_2} B_{n_2} D_{n_2} F_{n_2}$ near $F_{n_1} = F_{n_2}$ as in Figure 13. Our tetrahedra are all ideal, so the triangles $\triangle \alpha_1 \alpha_2 \alpha_3$ and $\triangle \alpha_1 \alpha_4 \alpha_5$ are Euclidean. Note that $\alpha_1, \dots, \alpha_5$ are points in the edges

⁴ Collapsing may identify some horizontal edges to non-horizontal edges. In this case, we put these identified edges in \mathcal{A} .

$A_{n_1}F_{n_1} = C_{n_2}F_{n_2}$, $B_{n_1}F_{n_1}$, $D_{n_1}F_{n_1}$, $D_{n_2}F_{n_2}$, $B_{n_2}F_{n_2}$ respectively. Furthermore, edges $\alpha_1\alpha_2$ and $\alpha_1\alpha_3$ are identified to $\alpha_1\alpha_5$ and $\alpha_1\alpha_4$ respectively.⁵ On the edge $A_{n_1}F_{n_1} = C_{n_2}F_{n_2}$, two shape parameters w_a/w_b and w_b/w_a are assigned respectively by the assigning rule, so the edge relation of $A_{n_1}F_{n_1} = C_{n_2}F_{n_2} \in \mathcal{B}$ holds trivially.

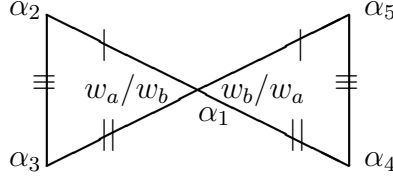


Figure 13: Part of the cusp diagram of Figure 12(a)

In the case of Figure 12(c), we want to prove the edge relation of $A_{n_1}F_{n_1} \in \mathcal{B}$ holds trivially. If n_2 is a positive crossing, we draw a part of the cusp diagram in $A_{n_1}B_{n_1}D_{n_1}F_{n_1} \cup A_{n_2}C_{n_2}D_{n_2}E_{n_2}$ near $F_{n_1} = E_{n_2}$, and if n_2 is a negative crossing, we draw a part of the cusp diagram in $A_{n_1}B_{n_1}D_{n_1}F_{n_1} \cup A_{n_2}B_{n_2}C_{n_2}E_{n_2}$ near $F_{n_1} = E_{n_2}$ as in Figure 14.

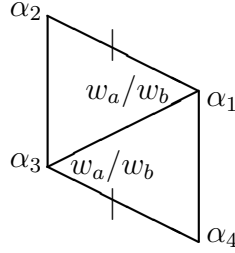


Figure 14: Part of the cusp diagram of Figure 12(c)

Note that if n_2 is a positive crossing, then $\alpha_1, \dots, \alpha_4$ are points in the edges $A_{n_1}F_{n_1} = A_{n_2}E_{n_2}$, $B_{n_1}F_{n_1}$, $D_{n_1}F_{n_1} = D_{n_2}E_{n_2}$, $C_{n_2}E_{n_2}$ respectively, and if n_2 is a negative crossing, then $\alpha_1, \dots, \alpha_4$ are points in the edges $A_{n_1}F_{n_1} = C_{n_2}E_{n_2}$, $B_{n_1}F_{n_1}$, $D_{n_1}F_{n_1} = B_{n_2}E_{n_2}$, $A_{n_2}E_{n_2}$ respectively. Furthermore, the edge $\alpha_2\alpha_1$ is identified to $\alpha_3\alpha_4$, so the diagram in Figure 14 becomes an annulus. The product of shape parameters around $\alpha_1 = \alpha_4$ in the annulus is $\frac{w_a}{w_b} \left(\frac{w_a}{w_b} \right)' \left(\frac{w_a}{w_b} \right)'' = -1$, and the one around $\alpha_2 = \alpha_3$ is also -1 . Therefore, if we consider the previous annulus on the right of Figure 14, which shares the edge $\alpha_1\alpha_4$, we obtain the edge relation of $A_{n_1}F_{n_1}$ trivially.

We remark that the previous annulus always exists because, when we follow the horizontal line in Figure 12(c) backwards, after meeting the under-crossing point n_2 , we let the next over-crossing point n_3 . (See Figure 15) (If n_3 does not exist, then $A_{n_1}F_{n_1} \in \mathcal{A}$ and it violates our assumption.) Then a part of the cusp diagram between n_2 and n_3 also forms an annulus, and this is the previous annulus.⁶

⁵ In fact, edges $\alpha_2\alpha_3$ and $\alpha_5\alpha_4$ are also identified, so the two triangles are cancelled each other. This means the corresponding tetrahedra $A_{n_1}B_{n_1}D_{n_1}F_{n_1}$ and $C_{n_2}B_{n_2}D_{n_2}F_{n_2}$ are cancelled each other.

⁶ As we seen in the case of Figure 12(a), the crossing points between n_2 and n_3 does not have any effect on the part of the cusp diagram because the triangles in Figure 13 cancelled each other. Also, as explained below, the existence of the previous annulus is still true even if some regions between n_2 and n_3 are unbounded.

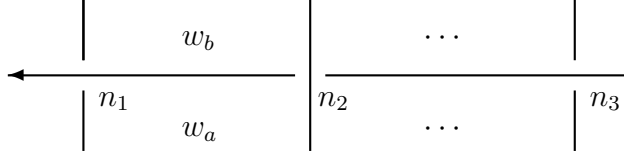


Figure 15: Previous annulus

The cases of Figure 12(b) and Figure 12(d) are the same with the cases of Figure 12(a) and Figure 12(c) respectively. Therefore, we find all the edges in \mathcal{B} satisfy the edge relations trivially by the method of parametrizing edges.

Now we assume one of the regions parametrized by w_a or w_b in Figure 12 is unbounded region. Then the cusp diagram in Figure 13 collapsed to an edge $\alpha_2\alpha_3 = \alpha_5\alpha_4$ and the one in Figure 14 collapsed to an edge $\alpha_2\alpha_3 = \alpha_1\alpha_4$. Therefore, our arguments for \mathcal{B} still hold for the collapsed case.⁷

□

Proof of Proposition 1.1. Consider the function $P_1(w_j, w_k, w_l, w_m)$, which was appeared in Section 3.2. By direct calculation, we obtain

$$\exp\left(w_j \frac{\partial P_1}{\partial w_j}\right) = \left(\frac{w_j w_l}{w_k w_m}\right)' \left(\frac{w_m}{w_j}\right)'' \left(\frac{w_k}{w_j}\right)'', \quad (7)$$

$$\exp\left(w_k \frac{\partial P_1}{\partial w_k}\right) = \left(\frac{w_j w_l}{w_k w_m}\right)'' \left(\frac{w_k}{w_l}\right)' \left(\frac{w_k}{w_j}\right)', \quad (8)$$

$$\exp\left(w_l \frac{\partial P_1}{\partial w_l}\right) = \left(\frac{w_j w_l}{w_k w_m}\right)' \left(\frac{w_m}{w_l}\right)'' \left(\frac{w_k}{w_l}\right)'', \quad (9)$$

$$\exp\left(w_m \frac{\partial P_1}{\partial w_m}\right) = \left(\frac{w_j w_l}{w_k w_m}\right)'' \left(\frac{w_m}{w_l}\right)' \left(\frac{w_m}{w_j}\right)'. \quad (10)$$

Note that (7), (8), (9) and (10) are the product of shape parameters assigned to the edges $C_n D_n$, $D_n A_n$, $A_n B_n$ and $B_n C_n$ of Figure 10(a) respectively.⁸ Also, after evaluating $w_l = 0$ to P_1 , we obtain

$$\exp\left(w_j \frac{\partial P_1(w_j, w_k, 0, w_m)}{\partial w_j}\right) = \left(\frac{w_m}{w_j}\right)'' \left(\frac{w_k}{w_j}\right)'', \quad (11)$$

$$\exp\left(w_k \frac{\partial P_1(w_j, w_k, 0, w_m)}{\partial w_k}\right) = \frac{w_m}{w_j} \left(\frac{w_k}{w_j}\right)', \quad (12)$$

$$\exp\left(w_m \frac{\partial P_1(w_j, w_k, 0, w_m)}{\partial w_m}\right) = \left(\frac{w_m}{w_j}\right)' \frac{w_k}{w_j}. \quad (13)$$

⁷ What we need is to consider the next annuli on the left and the right side, and do the same arguments.

⁸ For example, consider the equation (7) and Figure 10(a). The shape parameters assigned to the edge $C_n D_n$ are $\left(\frac{w_j w_l}{w_k w_m}\right)'$, $\left(\frac{w_m}{w_j}\right)''$ and $\left(\frac{w_k}{w_j}\right)''$, which come from the tetrahedra $C_n D_n A_n B_n$, $C_n D_n B_n F_n$ and $C_n D_n A_n E_n$ respectively.

Note that (11), (12) and (13) are the product of shape parameters assigned to the edges $C_n D_n$, $D_n A_n$ and $B_n C_n$ of Figure 10(a) respectively after collapsing the edge $A_n B_n$. Direct calculation shows the same relations hold for P_2 , P_3 , P_4 , N_1 , N_2 , N_3 and N_4 .

Consider the first potential function for the end point of I in Section 3.2. Direct calculation shows

$$\exp\left(w_l \frac{\partial P_1(w_j, w_j, w_l, w_m)}{\partial w_l}\right) = \exp\left(w_l \frac{\partial P_1(w_j, w_j, w_l, 0)}{\partial w_l}\right) = \left(\frac{w_j}{w_l}\right)'', \quad (14)$$

$$\exp\left(w_m \frac{\partial P_1(w_j, w_j, w_l, w_m)}{\partial w_m}\right) = \exp\left(w_m \frac{\partial P_1(w_j, w_j, 0, w_m)}{\partial w_m}\right) = \left(\frac{w_m}{w_j}\right)', \quad (15)$$

$$\exp\left(w_j \frac{\partial P_1(w_j, w_j, w_l, w_m)}{\partial w_j}\right) = \left(\frac{w_j}{w_m}\right)'' \left(\frac{w_l}{w_j}\right)' = \left(\frac{w_m}{w_j}\right)'' \left(\frac{w_j}{w_l}\right)' \frac{w_m}{w_l}, \quad (16)$$

$$\exp\left(w_j \frac{\partial P_1(w_j, w_j, 0, w_m)}{\partial w_j}\right) = \left(\frac{w_j}{w_m}\right)'' = \left(\frac{w_m}{w_j}\right)'' \frac{w_m}{w_j} (-1), \quad (17)$$

$$\exp\left(w_j \frac{\partial P_1(w_j, w_j, w_l, 0)}{\partial w_j}\right) = \left(\frac{w_l}{w_j}\right)' = \left(\frac{w_j}{w_l}\right)' \frac{w_j}{w_l} (-1), \quad (18)$$

where (14) and (15) are the product of shape parameters assigned to the edges $A_n B_n$ and $B_n C_n$ of Figure 10(a) after collapsing the edge $D_n E_n$ respectively without or with the collapsing of a horizontal edge.

To explain that (16), (17) and (18) are still parts of edge relations, we need different discussion. At first, see Figure 16.

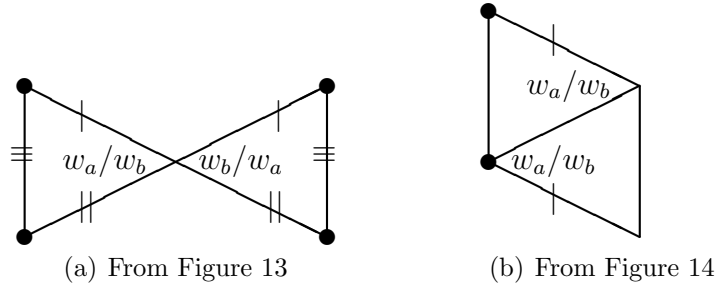


Figure 16: Parts of the cusp diagrams from Figure 13 and Figure 14

In Figure 16(a), the product of all shape parameters assigned to the edge expressed by dots is

$$\left(\frac{w_a}{w_b}\right)' \left(\frac{w_a}{w_b}\right)'' \left(\frac{w_b}{w_a}\right)' \left(\frac{w_b}{w_a}\right)'' = 1, \quad (19)$$

and in Figure 16(b), the product is

$$\left(\frac{w_a}{w_b}\right)' \left(\frac{w_a}{w_b}\right)'' \frac{w_a}{w_b} = -1. \quad (20)$$

To see the meaning of (16), consider the following two cases in Figure 17, where n_1 is the end point of I and n_2 is the previous over-crossing point. Figure 17(a) means the case when there is no crossing point between n_1 and n_2 , and Figure 17(b) means the other case.

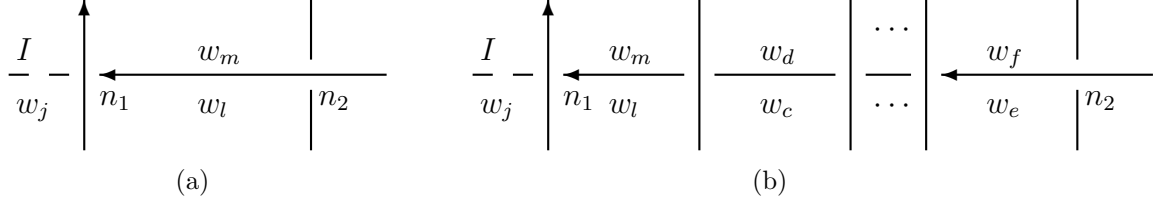


Figure 17: Two cases after the end point of I

Because n_1 is the end point of I , the edge $D_{n_1}E_{n_1}$ of the octahedron on n_1 in Figure 10(a) is collapsed to a point $D_{n_1} = E_{n_1}$ and it become two tetrahedra as in Figure 18. (If one more horizontal edge is collapsed here, the result becomes one tetrahedron. This is the cases of equations (17) and (18).)

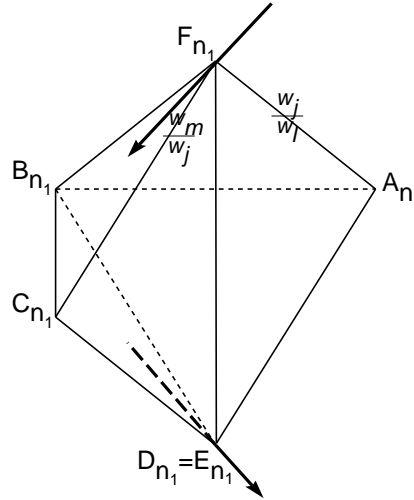


Figure 18: Figure 10(a) after collapsing the edge $D_{n_1}E_{n_1}$

The part of the cusp diagrams of each cases are in Figure 19. (See Figure 9 and Figure 10 for the assigning rule of the shape parameters.)

In the case of Figure 17(a), the product of shape parameters assigned to the edges $C_{n_1}D_{n_1} = D_{n_1}A_{n_1}$ of Figure 18 is $\left(\frac{w_m}{w_j}\right)''\left(\frac{w_j}{w_l}\right)'$. These edges are identified to $C_{n_2}F_{n_2}$, and $\frac{w_l}{w_m}$ is assigned to this edge. This explains that (16) is the product of shape parameters assigned to the edges $C_{n_1}D_{n_1} = D_{n_1}A_{n_1} = C_{n_2}F_{n_2}$.

In the case of Figure 17(b), the product of shape parameters assigned to the edges $C_{n_1}D_{n_1} = D_{n_1}A_{n_1}$ of Figure 18 is $\left(\frac{w_m}{w_j}\right)''\left(\frac{w_j}{w_i}\right)'$. In Figure 19(b), these edges are identified to the edges presented by the dots, and the product of shape parameters assigned to the

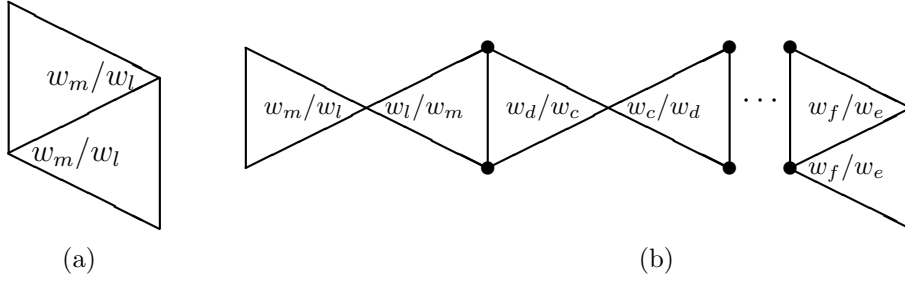


Figure 19: The parts of the cusp diagram corresponding to Figure 17

edges is

$$\left(\frac{w_l}{w_m}\right)' \left(\frac{w_l}{w_m}\right)'' \times 1 \times \cdots \times (-1) = \frac{w_m}{w_l}$$

by (19) and (20). This also explains (16) is the product of shape parameters assigned to $C_{n_1}D_{n_1} = D_{n_1}A_{n_1}$ and some other edges identified to this. This fact is still true⁹ even if some of the regions assigned by $w_c, w_d, \dots, w_e, w_f$ are unbounded regions, because the collapsing of the horizontal edges makes the cusp diagrams of Figure 13 and Figure 14 into edges. If the cusp diagram of Figure 13 becomes an edge, then ignoring the diagram is enough for our consideration, and if that of Figure 14 becomes an edge, then considering the previous annulus is enough. The previous annulus always exists because, by the same argument in the proof of Lemma 4.1, if we choose the next over-crossing point n_3 by following the horizontal lines backwards, the cusp diagram between n_2 and n_3 becomes the previous annulus.¹⁰

Now we describe the meaning of (17). Let n_1 be the end point of I , n_2 be the previous over-crossing point and n_3 be the previous under-crossing point. Also let \tilde{n} be the previous point of n_1 . Assume the edges $D_{n_1}E_{n_1}$ and $A_{n_1}B_{n_1}$ of Figure 10(a) are collapsed. Then $C_{n_1}D_{n_1} = B_{n_1}D_{n_1}$ and $\left(\frac{w_m}{w_j}\right)'' \frac{w_m}{w_j}$ is assigned to this edge. If $\tilde{n} = n_2$, then the edges identified to $C_{n_1}D_{n_1} = B_{n_1}D_{n_1}$ are appeared between the points $\tilde{n} = n_2$ and n_3 as the dots in Figure 16, and if $\tilde{n} \neq n_2$, then the edges are appeared between \tilde{n} and n_2 as the same way. Especially, Figure 16(a) may appear many times, but Figure 16(b) appears only one time at the point n_3 or n_2 respectively. By (19) and (20), the product of all shape parameters assigned to the dots is -1 , so (17) is the product of shape parameters assigned to the edges $C_{n_1}D_{n_1} = B_{n_1}D_{n_1}$ and some others identified to these. This fact is still true when some of the horizontal edges or non-horizontal edges of the octahedra are collapsed because of the same reason explained in the case of (16) before.

The same relations hold for (18) and the cases of other potential functions of the endpoints of I and J by the same arguments.

⁹ Even if the endpoint of J lies between the crossings n_1 and n_2 , this fact is still true because the collapsing of the non-horizontal edges does not change the part of the cusp diagram we are considering.

¹⁰ There is a concern that the previous annulus is collapsed to an edge, and all the previous annuli, following the horizontal line, are collapsed to edges. However, this cannot happen because Thurston triangulation is a triangulation of the hyperbolic knot complement $S^3 - K$ and we assumed the existence of the geometric solution.

Therefore, we conclude that \mathcal{H}_2 becomes all the edge relations of \mathcal{A} except the one horizontal edge whose region is assigned to 0 instead of the variables w_1, \dots, w_m . For an ideal tetrahedron parametrized with $u \in \mathbb{C}$ as in Figure 11, the product of all shape parameters assigned to all edges in the tetrahedron is $(uu'/u'')^2 = 1$. This implies the product of all edge relations becomes 1. On the other hand, from Lemma 4.1 and the above arguments, we found all but one edge relation by \mathcal{H}_2 . Therefore, the remaining edge relation holds automatically.

Finally, we prove \mathcal{H}_2 contains the cusp condition. Note that edges $\alpha_1\alpha_4$ and $\alpha_2\alpha_3$ in Figure 14 are meridians of the cusp diagram. The same shape parameter $\frac{w_a}{w_b}$ is assigned to the corners $\angle\alpha_2\alpha_1\alpha_3$ and $\angle\alpha_1\alpha_3\alpha_4$, so one of the cusp condition is trivially satisfied by the method of assigning shape parameters to edges. If we have all the edge relations and one cusp condition of a meridian, then we can obtain all the other cusp conditions using these relations. Therefore, we conclude \mathcal{H}_2 is the hyperbolicity equations of Thurston triangulation of $S^3 - K$. □

We remark one technical fact. For Thurston triangulation, let the shape parameters of the ideal tetrahedra be s_1, \dots, s_h . These parameters are defined by the ratios of a solution w_1, \dots, w_m of \mathcal{H}_2 , so if the values of w_1, \dots, w_m are fixed, then the values of s_1, \dots, s_h are uniquely determined and satisfy the hyperbolicity equation. Likewise, if the values of s_1, \dots, s_h satisfying the hyperbolicity equations are fixed, then we can uniquely determine the solution of w_1, \dots, w_m of \mathcal{H}_2 as follows: At first, we can determine some of the values of w_1, \dots, w_m , which are assigned to the regions adjacent to the region assigned with the number 0. Once a value w_l of a region is determined, then all the values of the adjacent regions can be determined. Therefore, all w_1, \dots, w_m can be determined. Furthermore, those values are well-defined and become a solution of \mathcal{H}_2 because of the hyperbolicity equations.

In next section, we will show the shape parameters of Yokota triangulation determines that of Thurston triangulation, and with certain restriction, vice versa. By the above discussion, this correspondence means each essential solution of \mathcal{H}_1 determines unique solution of \mathcal{H}_2 . Furthermore, if all the determined solutions of \mathcal{H}_2 are essential, then each essential solution of \mathcal{H}_2 determines unique essential solution of \mathcal{H}_1 .

5 Proof of Theorem 1.3

We start this section with the proof of Lemma 1.2.

Proof of Lemma 1.2. For a hyperbolic ideal octahedron in Figure 20, we assign shape parameters $t_1, t_2, t_3, t_4, u_1, u_2, u_3$ and u_4 to the edges CD, DA, AB, BC, CF, DE, AF and BE respectively. Let $u_5 := \frac{1}{u_1 u_3} = \frac{1}{u_2 u_4}$, which is also a shape parameter assigned to the edges AC and BD of the tetrahedron ABCD.

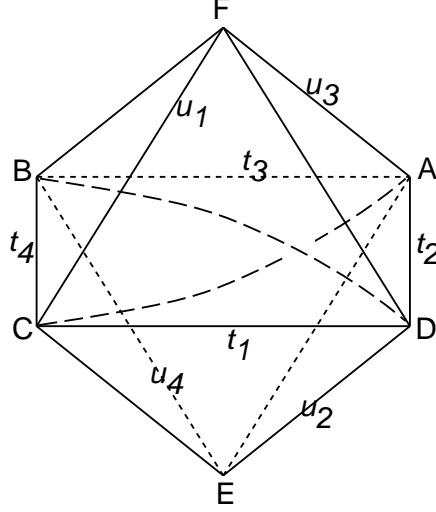


Figure 20: Assignment of shape parameters

Then we obtain the following relations.

$$\left\{ \begin{array}{l} u_1 = t'_1 t''_4, \\ u_2 = t'_1 t''_2, \\ u_3 = t'_3 t''_2, \\ u_4 = t'_3 t''_4, \\ u_5 = (t'_1 t''_2 t'_3 t''_4)^{-1}, \end{array} \right. \quad \left\{ \begin{array}{l} t_1 = u''_1 u''_2 u'_5, \\ t_2 = u'_2 u'_3 u''_5, \\ t_3 = u''_3 u''_4 u'_5, \\ t_4 = u'_4 u'_1 u''_5, \\ t_1 t_2 t_3 t_4 = 1. \end{array} \right. \quad (21)$$

Note that t_1, \dots, t_4 and u_1, \dots, u_5 are the shape parameters of tetrahedra in Yokota triangulation and Thurston triangulation respectively. According to Observation 2.1, we know these two triangulations are related by 3-2 moves and 4-5 moves on collapsed octahedra and non-collapsed octahedra respectively. The equation (21) shows the correspondence between the shape parameters under 4-5 moves, so if $t_1, \dots, t_4 \notin \{0, 1, \infty\}$, we can determine the values of u_1, \dots, u_5 from the left side of (21). Also the equation corresponding to 3-2 move can be obtained easily. (See (31) for example.) This implies that the shape parameters of Yokota triangulation determine that of Thurston triangulation. Furthermore, if all $u_1, \dots, u_5 \notin \{0, 1, \infty\}$, then the shape parameters of Thurston triangulation recovers that of Yokota triangulation by the right side of (21). It completes the proof. \square

Our goal of this section is to prove

$$V_0(z_1, \dots, z_g) \equiv W_0(w_1, \dots, w_m) \pmod{4\pi^2},$$

for any essential solution (z_1, \dots, z_g) of \mathcal{H}_1 and the corresponding essential solution (w_1, \dots, w_m) of \mathcal{H}_2 . To prove it, we introduce the dilogarithm identities of an ideal octahedron in Lemma 5.1. To avoid confusion, we assume the principal branch of the logarithm function.

Let $D(z) := \text{Im Li}_2(z) + \log |z| \arg(1-z)$ be the Bloch-Wigner function for $z \in \mathbb{C} - \{0, 1\}$. It is a well-known fact that $D(z) = \text{vol}(T_z)$, where T_z is the hyperbolic ideal tetrahedron with the shape parameter z . Therefore, from Figure 20, we obtain

$$D(t_1) + D(t_2) + D(t_3) + D(t_4) = D(u_1) + D(u_2) + D(u_3) + D(u_4) + D(u_5). \quad (22)$$

Lemma 5.1. *Let $t_1, t_2, t_3, t_4, u_1, u_2, u_3, u_4, u_5 \notin \{0, 1, \infty\}$ be the shape parameters defined in the hyperbolic octahedron in Figure 20, which are satisfying (21) and (22). Then the following identities hold.*

$$\begin{aligned} & \text{Li}_2(t_1) - \text{Li}_2\left(\frac{1}{t_2}\right) + \text{Li}_2(t_3) - \text{Li}_2\left(\frac{1}{t_4}\right) \\ &= \text{Li}_2(u_1) + \text{Li}_2(u_2) - \text{Li}_2\left(\frac{1}{u_3}\right) - \text{Li}_2\left(\frac{1}{u_4}\right) + \text{Li}_2(u_5) - \frac{\pi^2}{6} + \log u_1 \log u_2 \\ & \quad - \left(-\log(1-t_1) + \log(1-\frac{1}{t_4})\right) \log u_2 - \left(-\log(1-t_1) + \log(1-\frac{1}{t_2})\right) \log u_1 \\ & \quad + \left(-\log(1-t_1) + \log(1-\frac{1}{t_4})\right) \log(1-u_1) + \left(-\log(1-t_1) + \log(1-\frac{1}{t_2})\right) \log(1-u_2) \\ & \quad + \left(-\log(1-t_3) + \log(1-\frac{1}{t_2})\right) \log(1-\frac{1}{u_3}) + \left(-\log(1-t_3) + \log(1-\frac{1}{t_4})\right) \log(1-\frac{1}{u_4}) \\ & \quad + \left(\log(1-t_1) - \log(1-\frac{1}{t_2}) + \log(1-t_3) - \log(1-\frac{1}{t_4})\right) \log(1-u_5) \end{aligned} \quad (23)$$

$$\begin{aligned} &= \text{Li}_2(u_1) - \text{Li}_2\left(\frac{1}{u_2}\right) - \text{Li}_2\left(\frac{1}{u_3}\right) + \text{Li}_2(u_4) - \text{Li}_2\left(\frac{1}{u_5}\right) + \frac{\pi^2}{6} - \log u_2 \log u_3 \\ & \quad + \left(-\log(1-t_3) + \log(1-\frac{1}{t_2})\right) \log u_2 + \left(-\log(1-t_1) + \log(1-\frac{1}{t_2})\right) \log u_3 \\ & \quad + \left(-\log(1-t_1) + \log(1-\frac{1}{t_4})\right) \log(1-u_1) + \left(-\log(1-t_1) + \log(1-\frac{1}{t_2})\right) \log(1-\frac{1}{u_2}) \\ & \quad + \left(-\log(1-t_3) + \log(1-\frac{1}{t_2})\right) \log(1-\frac{1}{u_3}) + \left(-\log(1-t_3) + \log(1-\frac{1}{t_4})\right) \log(1-u_4) \\ & \quad + \left(\log(1-t_1) - \log(1-\frac{1}{t_2}) + \log(1-t_3) - \log(1-\frac{1}{t_4})\right) \log(1-\frac{1}{u_5}) \end{aligned} \quad (24)$$

$$\begin{aligned}
&= -\text{Li}_2\left(\frac{1}{u_1}\right) - \text{Li}_2\left(\frac{1}{u_2}\right) + \text{Li}_2(u_3) + \text{Li}_2(u_4) + \text{Li}_2(u_5) - \frac{\pi^2}{6} + \log u_3 \log u_4 \\
&\quad - \left(-\log(1-t_3) + \log\left(1 - \frac{1}{t_4}\right)\right) \log u_3 - \left(-\log(1-t_3) + \log\left(1 - \frac{1}{t_2}\right)\right) \log u_4 \\
&\quad + \left(-\log(1-t_1) + \log\left(1 - \frac{1}{t_4}\right)\right) \log\left(1 - \frac{1}{u_1}\right) + \left(-\log(1-t_1) + \log\left(1 - \frac{1}{t_2}\right)\right) \log\left(1 - \frac{1}{u_2}\right) \\
&\quad + \left(-\log(1-t_3) + \log\left(1 - \frac{1}{t_2}\right)\right) \log(1-u_3) + \left(-\log(1-t_3) + \log\left(1 - \frac{1}{t_4}\right)\right) \log(1-u_4) \\
&\quad + \left(\log(1-t_1) - \log\left(1 - \frac{1}{t_2}\right) + \log(1-t_3) - \log\left(1 - \frac{1}{t_4}\right)\right) \log(1-u_5)
\end{aligned} \tag{25}$$

$$\begin{aligned}
&= -\text{Li}_2\left(\frac{1}{u_1}\right) + \text{Li}_2(u_2) + \text{Li}_2(u_3) - \text{Li}_2\left(\frac{1}{u_4}\right) - \text{Li}_2\left(\frac{1}{u_5}\right) + \frac{\pi^2}{6} - \log u_1 \log u_4 \\
&\quad + \left(-\log(1-t_1) + \log\left(1 - \frac{1}{t_4}\right)\right) \log u_4 + \left(-\log(1-t_3) + \log\left(1 - \frac{1}{t_4}\right)\right) \log u_1 \\
&\quad + \left(-\log(1-t_1) + \log\left(1 - \frac{1}{t_4}\right)\right) \log\left(1 - \frac{1}{u_1}\right) + \left(-\log(1-t_1) + \log\left(1 - \frac{1}{t_2}\right)\right) \log(1-u_2) \\
&\quad + \left(-\log(1-t_3) + \log\left(1 - \frac{1}{t_2}\right)\right) \log(1-u_3) + \left(-\log(1-t_3) + \log\left(1 - \frac{1}{t_4}\right)\right) \log\left(1 - \frac{1}{u_4}\right) \\
&\quad + \left(\log(1-t_1) - \log\left(1 - \frac{1}{t_2}\right) + \log(1-t_3) - \log\left(1 - \frac{1}{t_4}\right)\right) \log\left(1 - \frac{1}{u_5}\right).
\end{aligned} \tag{26}$$

Furthermore,

$$\begin{aligned}
\text{Li}_2(t_1) - \text{Li}_2\left(\frac{1}{t_2}\right) - \text{Li}_2\left(\frac{1}{t_4}\right) + \frac{\pi^2}{6} &= \text{Li}_2(u_1) + \text{Li}_2(u_2) - \frac{\pi^2}{6} + \log u_1 \log u_2 \\
&\quad + \left(-\log(1-t_1) + \log\left(1 - \frac{1}{t_4}\right)\right) (-\log u_2 + \log(1-u_1)) \\
&\quad + \left(-\log(1-t_1) + \log\left(1 - \frac{1}{t_2}\right)\right) (-\log u_1 + \log(1-u_2))
\end{aligned} \tag{27}$$

when CD is collapsed to a point,

$$\begin{aligned}
\text{Li}_2(t_1) - \text{Li}_2\left(\frac{1}{t_2}\right) + \text{Li}_2(t_3) - \frac{\pi^2}{6} &= -\text{Li}_2\left(\frac{1}{u_2}\right) - \text{Li}_2\left(\frac{1}{u_3}\right) + \frac{\pi^2}{6} - \log u_2 \log u_3 \\
&\quad + \left(-\log(1-t_3) + \log\left(1 - \frac{1}{t_2}\right)\right) \left(\log u_2 + \log\left(1 - \frac{1}{u_3}\right)\right) \\
&\quad + \left(-\log(1-t_1) + \log\left(1 - \frac{1}{t_2}\right)\right) \left(\log u_3 + \log\left(1 - \frac{1}{u_2}\right)\right)
\end{aligned} \tag{28}$$

when DA is collapsed to a point,

$$\begin{aligned}
-\operatorname{Li}_2\left(\frac{1}{t_2}\right) + \operatorname{Li}_2(t_3) - \operatorname{Li}_2\left(\frac{1}{t_4}\right) + \frac{\pi^2}{6} &= \operatorname{Li}_2(u_3) + \operatorname{Li}_2(u_4) - \frac{\pi^2}{6} + \log u_3 \log u_4 \\
&+ \left(-\log(1-t_3) + \log\left(1 - \frac{1}{t_4}\right)\right) (-\log u_3 + \log(1-u_4)) \\
&+ \left(-\log(1-t_3) + \log\left(1 - \frac{1}{t_2}\right)\right) (-\log u_4 + \log(1-u_3))
\end{aligned} \tag{29}$$

when AB is collapsed to a point, and

$$\begin{aligned}
\operatorname{Li}_2(t_1) + \operatorname{Li}_2(t_3) - \operatorname{Li}_2\left(\frac{1}{t_4}\right) - \frac{\pi^2}{6} &= -\operatorname{Li}_2\left(\frac{1}{u_1}\right) - \operatorname{Li}_2\left(\frac{1}{u_4}\right) + \frac{\pi^2}{6} - \log u_1 \log u_4 \\
&+ \left(-\log(1-t_1) + \log\left(1 - \frac{1}{t_4}\right)\right) \left(\log u_4 + \log\left(1 - \frac{1}{u_1}\right)\right) \\
&+ \left(-\log(1-t_3) + \log\left(1 - \frac{1}{t_4}\right)\right) \left(\log u_1 + \log\left(1 - \frac{1}{u_4}\right)\right)
\end{aligned} \tag{30}$$

when BC is collapsed to a point.

Proof. After the direct calculation of the imaginary parts of (23), (24), (25), (26), they coincide with

$$\begin{aligned}
D(t_1) - D\left(\frac{1}{t_2}\right) + D(t_3) - D\left(\frac{1}{t_4}\right) &= D(u_1) + D(u_2) - D\left(\frac{1}{u_3}\right) - D\left(\frac{1}{u_4}\right) + D(u_5), \\
D(t_1) - D\left(\frac{1}{t_2}\right) + D(t_3) - D\left(\frac{1}{t_4}\right) &= D(u_1) - D\left(\frac{1}{u_2}\right) - D\left(\frac{1}{u_3}\right) + D(u_4) - D\left(\frac{1}{u_5}\right), \\
D(t_1) - D\left(\frac{1}{t_2}\right) + D(t_3) - D\left(\frac{1}{t_4}\right) &= -D\left(\frac{1}{u_1}\right) - D\left(\frac{1}{u_2}\right) + D(u_3) + D(u_4) + D(u_5), \\
D(t_1) - D\left(\frac{1}{t_2}\right) + D(t_3) - D\left(\frac{1}{t_4}\right) &= -D\left(\frac{1}{u_1}\right) + D(u_2) + D(u_3) - D\left(\frac{1}{u_4}\right) - D\left(\frac{1}{u_5}\right),
\end{aligned}$$

respectively by the definition of D and (21). Each of these identities are equivalent to (22) by the well-known fact $D(\frac{1}{z}) = -D(z)$, so the imaginary parts of (23), (24), (25), (26) hold.

For example, the imaginary part of (23) becomes

$$\begin{aligned}
& D(t_1) - D\left(\frac{1}{t_2}\right) + D(t_3) - D\left(\frac{1}{t_4}\right) - \log |t_1| \arg(1 - t_1) \\
& \quad - \log |t_2| \arg\left(1 - \frac{1}{t_2}\right) - \log |t_3| \arg(1 - t_3) - \log |t_4| \arg\left(1 - \frac{1}{t_4}\right) \\
& = D(u_1) + D(u_2) - D\left(\frac{1}{u_3}\right) - D\left(\frac{1}{u_4}\right) + D(u_5) + \log |u_1| \arg u_2 + \arg u_1 \log |u_2| \\
& \quad - \log |u_1| \arg(1 - u_1) - \log |u_2| \arg(1 - u_2) - \log |u_3| \arg\left(1 - \frac{1}{u_3}\right) \\
& \quad - \log |u_4| \arg\left(1 - \frac{1}{u_4}\right) - \log |u_5| \arg(1 - u_5) \\
& \quad - \log |u_1| \arg u_2 - \log |u_2| \arg u_1 \\
& \quad + \log |u_1| \arg(1 - u_1) + \log |u_2| \arg(1 - u_2) + \log |u_3| \arg\left(1 - \frac{1}{u_3}\right) \\
& \quad + \log |u_4| \arg\left(1 - \frac{1}{u_4}\right) + \log |u_5| \arg(1 - u_5) \\
& \quad - \arg(1 - t_1) \log \left| u_2^{-1} u_1^{-1} (1 - u_1)(1 - u_2)(1 - u_5)^{-1} \right| \\
& \quad - \arg\left(1 - \frac{1}{t_2}\right) \log \left| u_1(1 - u_2)^{-1} \left(1 - \frac{1}{u_3}\right)^{-1} (1 - u_5) \right| \\
& \quad - \arg(1 - t_3) \log \left| \left(1 - \frac{1}{u_3}\right) \left(1 - \frac{1}{u_4}\right) (1 - u_5)^{-1} \right| \\
& \quad - \arg\left(1 - \frac{1}{t_4}\right) \log \left| u_2(1 - u_1)^{-1} \left(1 - \frac{1}{u_4}\right)^{-1} (1 - u_5) \right|.
\end{aligned}$$

Using $u_5 = \frac{1}{u_1 u_3} = \frac{1}{u_2 u_4}$, we obtain

$$\begin{aligned}
u_1(1 - u_2)^{-1} \left(1 - \frac{1}{u_3}\right)^{-1} (1 - u_5) &= u_2' u_3' u_5'' = t_2, \\
u_2(1 - u_1)^{-1} \left(1 - \frac{1}{u_4}\right)^{-1} (1 - u_5) &= u_4' u_1' u_5'' = t_4.
\end{aligned}$$

Applying them, we can check the imaginary part of (23) is equivalent to (22).

On the other hand, (23), (24), (25), (26) are analytic functions on certain 3-dimensional open set, so the real parts also hold up to some real constants. After evaluating $t_1 = t_2 = t_3 = t_4 = u_1 = u_2 = u_3 = u_4 = i$ and $u_5 = -1$ to these functions,¹¹ we find that all constants are zero.

Now we assume the edge CD is collapsed to a point. Then we obtain the following

¹¹ Note that $\text{Li}_2(-1) = -\frac{\pi^2}{12}$.

relations.

$$\begin{cases} u_1 = t'_1 t''_4, \\ u_2 = t'_1 t''_2, \end{cases} \begin{cases} t_1 = u''_1 u''_2, \\ t_2 = u_1 u'_2, \\ t_4 = u'_1 u_2, \\ t_1 t_2 t_4 = 1. \end{cases} \quad (31)$$

After the direct calculation of the imaginary part of (27), it coincides with

$$D(t_1) - D\left(\frac{1}{t_2}\right) - D\left(\frac{1}{t_4}\right) = D(u_1) + D(u_2)$$

by (31), and it holds by the additivity of volume. Because of the analyticity of (27) on certain 2-dimensional open set, the real part of (27) also holds up to a real constant. Evaluating $t_1 = t_2 = t_4 = \exp(\frac{2\pi i}{3})$ and $u_1 = u_2 = \exp(\frac{\pi i}{3})$ shows the constant is zero, so the identity (27) is true. Other identities (28), (29), (30) can be proved by the same method. \square

Proof of Theorem 1.3. Now we prove the theorem by calculating the potential functions on each crossing n . At first, consider the case that no edge of the octahedron on the positive crossing n is collapsed. Let the variables assigned to the contributing sides be z_a, \dots, z_d as in Figure 9 and let $t_1 = \frac{z_b}{z_a}$, $t_2 = \frac{z_c}{z_b}$, $t_3 = \frac{z_d}{z_c}$, $t_4 = \frac{z_a}{z_d}$ as in Figure 10(a). Then the Yokota potential function of the crossing becomes

$$X(z_a, \dots, z_d) := \text{Li}_2(t_1) - \text{Li}_2\left(\frac{1}{t_2}\right) + \text{Li}_2(t_3) - \text{Li}_2\left(\frac{1}{t_4}\right)$$

and

$$\begin{aligned} X_0(z_a, \dots, z_d) &= \text{Li}_2(t_1) - \text{Li}_2\left(\frac{1}{t_2}\right) + \text{Li}_2(t_3) - \text{Li}_2\left(\frac{1}{t_4}\right) \\ &+ \left(-\log(1 - t_1) + \log\left(1 - \frac{1}{t_4}\right)\right) \log z_a - \left(-\log(1 - t_1) + \log\left(1 - \frac{1}{t_2}\right)\right) \log z_b \\ &+ \left(-\log(1 - t_3) + \log\left(1 - \frac{1}{t_2}\right)\right) \log z_c - \left(-\log(1 - t_3) + \log\left(1 - \frac{1}{t_4}\right)\right) \log z_d. \end{aligned} \quad (32)$$

Likewise, let the variables assigned to the regions be w_j, \dots, w_m as in Figure 9 and let $u_1 = \frac{w_m}{w_j}$, $u_2 = \frac{w_k}{w_j}$, $u_3 = \frac{w_k}{w_l}$, $u_4 = \frac{w_m}{w_l}$, $u_5 = \frac{w_j w_l}{w_k w_m}$ as in Figure 10(a). Then the potential function of the colored Jones polynomial of the crossing becomes P_f , which was defined in

Lemma 3.1 for $f = 1, \dots, 4$, and

$$\begin{aligned}
P_{10} = & \operatorname{Li}_2(u_1) + \operatorname{Li}_2(u_2) - \operatorname{Li}_2\left(\frac{1}{u_3}\right) - \operatorname{Li}_2\left(\frac{1}{u_4}\right) + \operatorname{Li}_2(u_5) - \frac{\pi^2}{6} + \log u_1 \log u_2 \quad (33) \\
& + (-\log(1 - u_1) - \log(1 - u_2) + \log(1 - u_5) + \log u_1 + \log u_2) \log w_j \\
& + \left(\log(1 - u_2) + \log\left(1 - \frac{1}{u_3}\right) - \log(1 - u_5) - \log u_1 \right) \log w_k \\
& + \left(-\log\left(1 - \frac{1}{u_3}\right) - \log\left(1 - \frac{1}{u_4}\right) + \log(1 - u_5) \right) \log w_l \\
& + \left(\log(1 - u_1) + \log\left(1 - \frac{1}{u_4}\right) - \log(1 - u_5) - \log u_2 \right) \log w_m.
\end{aligned}$$

We define *the remaining term* Z_n by the difference of two potential functions $V_0 - W_0$ of the crossing n . In this case, $Z_n = X_0 - P_{10}$.

Assume $z_a, \dots, z_d, w_j, \dots, w_m$ satisfy the assumption of Lemma 5.1.¹² Let

$$\begin{cases} U_1 := -\log(1 - t_1) + \log\left(1 - \frac{1}{t_4}\right), \\ U_2 := -\log(1 - t_1) + \log\left(1 - \frac{1}{t_2}\right), \\ U_3 := -\log(1 - t_3) + \log\left(1 - \frac{1}{t_2}\right), \\ U_4 := -\log(1 - t_3) + \log\left(1 - \frac{1}{t_4}\right), \end{cases}
\begin{cases} T_1 := \log(1 - u_1) + \log(1 - u_2) - \log(1 - u_5) - \log u_1 - \log u_2, \\ T_2 := -\log(1 - u_2) - \log\left(1 - \frac{1}{u_3}\right) + \log(1 - u_5) + \log u_1, \\ T_3 := \log\left(1 - \frac{1}{u_3}\right) + \log\left(1 - \frac{1}{u_4}\right) - \log(1 - u_5), \\ T_4 := -\log(1 - u_1) - \log\left(1 - \frac{1}{u_4}\right) + \log(1 - u_5) + \log u_2. \end{cases}$$

Then, by (21),

$$\begin{cases} U_1 \equiv \log u_1 \equiv \log w_m - \log w_j \pmod{2\pi i}, \\ U_2 \equiv \log u_2 \equiv \log w_k - \log w_j \pmod{2\pi i}, \\ U_3 \equiv \log u_3 \equiv \log w_k - \log w_l \pmod{2\pi i}, \\ U_4 \equiv \log u_4 \equiv \log w_m - \log w_l \pmod{2\pi i}, \end{cases}
\begin{cases} T_1 \equiv \log t_1 \equiv \log z_b - \log z_a \pmod{2\pi i}, \\ T_2 \equiv \log t_2 \equiv \log z_c - \log z_b \pmod{2\pi i}, \\ T_3 \equiv \log t_3 \equiv \log z_d - \log z_c \pmod{2\pi i}, \\ T_4 \equiv \log t_4 \equiv \log z_a - \log z_d \pmod{2\pi i}, \end{cases}$$

and $U_1 + U_3 = U_2 + U_4$, $T_1 + T_2 + T_3 + T_4 = 0$. Applying these and (23) to (32) and (33), we

¹² Any essential solution (z_a, \dots, z_d) of \mathcal{H}_1 and the corresponding essential solution (w_j, \dots, w_m) of \mathcal{H}_2 satisfy this assumption.

obtain the remaining term Z_n of the crossing n as follows.

$$\begin{aligned}
Z_n &= X_0 - P_{10} = U_1 \log z_a - U_2 \log z_b + U_3 \log z_c - U_4 \log z_d \\
&\quad + T_1 \log w_j + T_2 \log w_k + T_3 \log w_l + T_4 \log w_m - U_1 \log u_2 - U_2 \log u_1 \\
&\quad + U_1 \log(1 - u_1) + U_2 \log(1 - u_2) + U_3 \log(1 - \frac{1}{u_3}) + U_4 \log(1 - \frac{1}{u_4}) - (U_1 + U_3) \log(1 - u_5) \\
&= T_1 \log w_j + T_2 \log w_k + T_3 \log w_l + T_4 \log w_m \\
&\quad + U_1 \left(\log z_a - \log z_d + \log(1 - u_1) + \log(1 - \frac{1}{u_4}) - \log(1 - u_5) - \log u_2 \right) \\
&\quad + U_2 \left(-\log z_b + \log z_d + \log(1 - u_2) - \log(1 - \frac{1}{u_4}) - \log u_1 \right) \\
&\quad + U_3 \left(\log z_c - \log z_d + \log(1 - \frac{1}{u_3}) + \log(1 - \frac{1}{u_4}) - \log(1 - u_5) \right) \\
&= T_2(\log w_k - \log w_j) + T_3(\log w_l - \log w_j) + T_4(\log w_m - \log w_j) \\
&\quad + U_1(\log z_a - \log z_d - T_4) + U_2(-\log z_b + \log z_d - T_2 - T_3) + U_3(\log z_c - \log z_d + T_3) \\
&\equiv T_2(\log w_k - \log w_j) + T_3(\log w_l - \log w_j) + T_4(\log w_m - \log w_j) \\
&\quad + (\log w_m - \log w_j)(\log z_a - \log z_d - T_4) + (\log w_k - \log w_j)(-\log z_b + \log z_d - T_2 - T_3) \\
&\quad + (\log w_k - \log w_l)(\log z_c - \log z_d + T_3) \pmod{4\pi^2} \\
&= -(\log w_j - \log w_m) \log z_a - (\log w_k - \log w_j) \log z_b + (\log w_k - \log w_l) \log z_c \\
&\quad + (\log w_l - \log w_m) \log z_d.
\end{aligned}$$

By the same method, we can prove that the remaining term of the negative crossing in Figure 9 is the same with that of the positive crossing.

Now we consider the case that only one horizontal edge is collapsed in an octahedron on a positive crossing n . Let the region assigned to r_l be the unbounded region and $z_c = z_d = 1$ in Figure 9. Also let $t_1 = \frac{z_b}{z_a}$, $t_2 = \frac{1}{z_b}$, $t_4 = z_a$ and $u_1 = \frac{w_m}{w_j}$, $u_2 = \frac{w_k}{w_j}$. Then the Yokota potential function of the crossing becomes

$$X(z_a, z_b) := \text{Li}_2(t_1) - \text{Li}_2(\frac{1}{t_2}) - \text{Li}_2(\frac{1}{t_4}) + \frac{\pi^2}{6}$$

and

$$\begin{aligned}
X_0(z_a, z_b) &= \text{Li}_2(t_1) - \text{Li}_2(\frac{1}{t_2}) - \text{Li}_2(\frac{1}{t_4}) + \frac{\pi^2}{6} \\
&\quad + \left(-\log(1 - t_1) + \log(1 - \frac{1}{t_4}) \right) \log z_a - \left(-\log(1 - t_1) + \log(1 - \frac{1}{t_2}) \right) \log z_b.
\end{aligned} \tag{34}$$

The potential function of the colored Jones polynomial of the crossing becomes

$$Y(w_j, w_k, w_m) := P_1(w_j, w_k, 0, w_m) = \text{Li}_2(u_1) + \text{Li}_2(u_2) - \frac{\pi^2}{6} + \log u_1 \log u_2$$

and

$$\begin{aligned}
Y_0(w_j, w_k, w_m) &= \text{Li}_2(u_1) + \text{Li}_2(u_2) - \frac{\pi^2}{6} + \log u_1 \log u_2 \\
&+ (-\log(1 - u_1) - \log(1 - u_2) + \log u_1 + \log u_2) \log w_j \\
&+ (\log(1 - u_2) - \log u_1) \log w_k + (\log(1 - u_1) - \log u_2) \log w_m.
\end{aligned} \tag{35}$$

In this case, the remaining term is $Z_n = X_0 - Y_0$. Let

$$\begin{cases} U_1 := -\log(1 - t_1) + \log(1 - \frac{1}{t_4}), \\ U_2 := -\log(1 - t_1) + \log(1 - \frac{1}{t_2}), \\ T_1 := \log(1 - u_1) + \log(1 - u_2) - \log u_1 - \log u_2, \\ T_2 := -\log(1 - u_2) + \log u_1, \\ T_4 := -\log(1 - u_1) + \log u_2. \end{cases}$$

Then, by (31),

$$\begin{cases} U_1 \equiv \log u_1 \equiv \log w_m - \log w_j \pmod{2\pi i}, \\ U_2 \equiv \log u_2 \equiv \log w_k - \log w_j \pmod{2\pi i}, \end{cases} \quad \begin{cases} T_1 \equiv \log t_1 \equiv \log z_b - \log z_a \pmod{2\pi i}, \\ T_2 \equiv \log t_2 \equiv -\log z_b \pmod{2\pi i}, \\ T_4 \equiv \log t_4 \equiv \log z_a \pmod{2\pi i}, \end{cases}$$

and $T_1 + T_2 + T_4 = 0$. Applying these and (27) to (34) and (35), we obtain the remaining term Z_n as follows.

$$\begin{aligned}
Z_n &= X_0 - Y_0 = U_1 \log z_a - U_2 \log z_b + T_1 \log w_j + T_2 \log w_k + T_4 \log w_m - U_1 T_4 - U_2 T_2 \\
&= U_1 \log z_a - U_2 \log z_b + T_2 (\log w_k - \log w_j - U_2) + T_4 (\log w_m - \log w_j - U_1) \\
&\equiv U_1 \log z_a - U_2 \log z_b \\
&\quad - \log z_b (\log w_k - \log w_j - U_2) + \log z_a (\log w_m - \log w_j - U_1) \pmod{4\pi^2} \\
&= -(\log w_j - \log w_m) \log z_a - (\log w_k - \log w_j) \log z_b.
\end{aligned}$$

By the same method, we can prove the remaining term of the negative crossing in this case is the same with that of the positive crossing. On the other hand, the remaining term becomes

$$Z_n = -(\log w_k - \log w_j) \log z_b + (\log w_k - \log w_l) \log z_c$$

when the region assigned to w_m is the unbounded region,

$$Z_n = (\log w_k - \log w_l) \log z_c + (\log w_l - \log w_m) \log z_d$$

when the region assigned to w_j is the unbounded region, and

$$Z_n = -(\log w_j - \log w_m) \log z_a + (\log w_l - \log w_m) \log z_d$$

when the region assigned to w_k is the unbounded region.

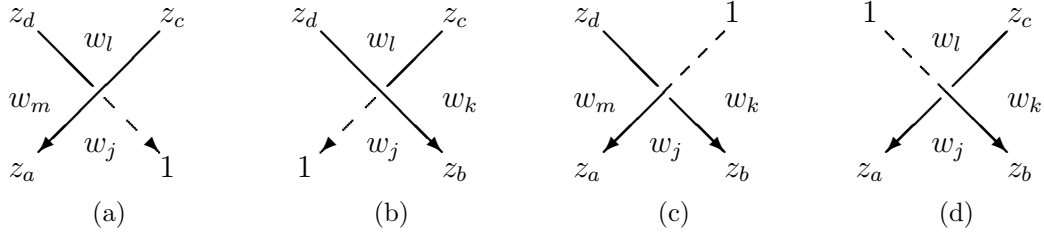


Figure 21: Four cases of the end point of I or J

Now we consider the case that the crossing point n is the endpoint of I or J . There are four cases as in Figure 21. We only prove the case of Figure 21(a) because the others can be proved by the same method.

At first, we assume all three regions in Figure 21(a) are bounded. Then, in Figure 10(a), the edge $B_n E_n$ is collapsed to a point and $\frac{z_d}{z_c}$, $\frac{z_a}{z_d}$, $\frac{w_m}{w_j}$, $\frac{w_l}{w_l}$ are assigned to the edges $C_n D_n$, $D_n A_n$, $A_n F_n$, $C_n F_n$ respectively. Also we obtain

$$\frac{z_d}{z_c} = \left(\frac{w_j}{w_l} \right)'' = 1 - \frac{w_l}{w_j} \quad \text{and} \quad \frac{w_m}{w_j} = \left(\frac{z_a}{z_d} \right)'' = 1 - \frac{z_d}{z_a}. \quad (36)$$

Applying (36) to Yokota potential function $X(z_a, z_c, z_d) := \text{Li}_2\left(\frac{z_d}{z_c}\right) - \text{Li}_2\left(\frac{z_d}{z_a}\right)$, we obtain

$$\begin{aligned} X_0 &= \text{Li}_2\left(\frac{z_d}{z_c}\right) - \text{Li}_2\left(\frac{z_d}{z_a}\right) + \log\left(1 - \frac{z_d}{z_a}\right) \log z_a - \log\left(1 - \frac{z_d}{z_c}\right) \log z_c \\ &\quad - \left(-\log\left(1 - \frac{z_d}{z_c}\right) + \log\left(1 - \frac{z_d}{z_a}\right) \right) \log z_d \\ &= \text{Li}_2\left(\frac{z_d}{z_c}\right) - \text{Li}_2\left(1 - \frac{w_m}{w_j}\right) + \log \frac{w_m}{w_j} (\log z_a - \log z_d) + \log \frac{w_l}{w_j} (\log z_d - \log z_c). \end{aligned}$$

Also, applying (36) to the potential function of the colored Jones polynomial $Y(w_j, w_l, w_m) := P_1(w_j, w_j, w_l, w_m) = \text{Li}_2\left(\frac{w_m}{w_j}\right) - \text{Li}_2\left(\frac{w_l}{w_j}\right)$, we obtain

$$\begin{aligned} Y_0 &= \text{Li}_2\left(\frac{w_m}{w_j}\right) - \text{Li}_2\left(\frac{w_l}{w_j}\right) - \left(\log\left(1 - \frac{w_m}{w_j}\right) - \log\left(1 - \frac{w_l}{w_j}\right) \right) \log w_j \\ &\quad - \log\left(1 - \frac{w_l}{w_j}\right) \log w_l + \log\left(1 - \frac{w_m}{w_j}\right) \log w_m \\ &= \text{Li}_2\left(\frac{w_m}{w_j}\right) - \text{Li}_2\left(1 - \frac{z_d}{z_c}\right) - \log \frac{z_d}{z_a} (\log w_j - \log w_m) - \log \frac{z_d}{z_c} (\log w_l - \log w_j). \end{aligned}$$

Using the well-known identity $\text{Li}_2(z) + \text{Li}_2(1 - z) = \frac{\pi^2}{6} - \log z \log(1 - z)$ for $z \in \mathbb{C} - \{0, 1\}$

in [5], we obtain the remaining term

$$\begin{aligned}
Z_n &= X_0 - Y_0 = -\log \frac{z_d}{z_c} \log \frac{w_l}{w_j} + \log \frac{w_m}{w_j} \log \frac{z_d}{z_a} \\
&\quad + \log \frac{w_m}{w_j} (\log z_a - \log z_d) + \log \frac{w_l}{w_j} (\log z_d - \log z_c) \\
&\quad + \log \frac{z_d}{z_a} (\log w_j - \log w_m) + \log \frac{z_d}{z_c} (\log w_l - \log w_j) \\
&= \log \frac{w_l}{w_j} \left(-\log \frac{z_d}{z_c} + \log z_d - \log z_c \right) + \log \frac{w_m}{w_j} \left(\log \frac{z_d}{z_a} + \log z_a - \log z_d \right) \\
&\quad + \log \frac{z_d}{z_a} (\log w_j - \log w_m) + \log \frac{z_d}{z_c} (\log w_l - \log w_j) \\
&\equiv (\log w_l - \log w_j) \left(-\log \frac{z_d}{z_c} + \log z_d - \log z_c \right) \\
&\quad + (\log w_m - \log w_j) \left(\log \frac{z_d}{z_a} + \log z_a - \log z_d \right) \\
&\quad + \log \frac{z_d}{z_a} (\log w_j - \log w_m) + \log \frac{z_d}{z_c} (\log w_l - \log w_j) \pmod{4\pi^2} \\
&= -(\log w_j - \log w_m) \log z_a + (\log w_j - \log w_l) \log z_c + (\log w_l - \log w_m) \log z_d.
\end{aligned}$$

Finally, we consider the case that the region assigned with w_l in Figure 21(a) is unbounded. Then the edges $B_n E_n$ and $C_n D_n$ are collapsed to points. Furthermore, $z_c = z_d = 1$ and $w_l = 0$, and $z_a, \frac{w_m}{w_j}$ are assigned to the edges $D_n A_n, A_n F_n$ in Figure 10(a) respectively. Applying

$$\frac{w_m}{w_j} = z_a'' = 1 - \frac{1}{z_a}$$

to Yokota potential function $X(z_a) := -\text{Li}_2(\frac{1}{z_a}) + \frac{\pi^2}{6}$, we obtain

$$X_0 = -\text{Li}_2\left(\frac{1}{z_a}\right) + \frac{\pi^2}{6} + \log\left(1 - \frac{1}{z_a}\right) \log z_a = -\text{Li}_2\left(\frac{1}{z_a}\right) + \frac{\pi^2}{6} + \log \frac{w_m}{w_j} \log z_a,$$

and to the potential function of the colored Jones polynomial $Y(w_j, w_m) := P_1(w_j, w_j, 0, w_m) = \text{Li}_2(\frac{w_m}{w_j})$, we obtain

$$Y_0 = \text{Li}_2\left(\frac{w_m}{w_j}\right) + \log\left(1 - \frac{w_m}{w_j}\right) (\log w_m - \log w_j) = \text{Li}_2\left(1 - \frac{1}{z_a}\right) + \log \frac{1}{z_a} (\log w_m - \log w_j).$$

Therefore, we obtain the remaining term

$$\begin{aligned}
Z_n &:= X_0 - Y_0 = \log \frac{1}{z_a} \log \frac{w_m}{w_j} + \log \frac{w_m}{w_j} \log z_a - \log \frac{1}{z_a} (\log w_m - \log w_j) \\
&= \log \frac{1}{z_a} (\log \frac{w_m}{w_j} - \log w_m + \log w_j) + \log \frac{w_m}{w_j} \log z_a \\
&\equiv -\log z_a (\log \frac{w_m}{w_j} - \log w_m + \log w_j) + \log \frac{w_m}{w_j} \log z_a \pmod{4\pi^2} \\
&= -(\log w_j - \log w_m) \log z_a.
\end{aligned}$$

Likewise, we can show the remaining term becomes

$$Z_n = (\log w_l - \log w_m) \log z_d$$

when the region assigned to w_m in Figure 21(a) is unbounded, and other three cases in Figure 21 can be obtained by the same method.

We complete the proof by proving

$$\sum_{n : \text{crossings of } G} Z_n = 0.$$

Note that we defined a contributing side of G in Section 3.1. Assume the side assigned by z_a in Figure 22 is a contributing side of G . (It means $z_a \neq 1$.)

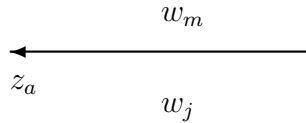


Figure 22: Contributing side assigned by z_a

If the side goes out of the crossing point n_1 , then the coefficient of $\log z_a$ in Z_{n_1} is $-(\log w_j - \log w_l)$, and if the side goes into the crossing point n_2 , then the coefficient of $\log z_a$ in Z_{n_2} is $(\log w_j - \log w_l)$. They are cancelled each other, and it happens for all the contributing sides. \square

A Appendix

A.1 Formal substitution of the colored Jones polynomial and the potential function

In this Appendix, we induce the potential function $W(w_1, \dots, w_m)$ defined in Section 3.2 from the formal substitution (1) of the colored Jones polynomial.

The colored Jones polynomial is determined by the R-matrix and the local maxima/minima. (See [7] for a reference.) However, as seen in (1), the local maxima/minima does not have an effect on the formal substitution. So we only consider the R-matrix of the colored Jones polynomial:

$$\begin{aligned} R_{l,m}^{j,k} &= \delta_{m,j-h} \delta_{l,k+h} \frac{(q^{-1})_j (q^{-1})_k^{-1}}{(q^{-1})_h (q^{-1})_l^{-1} (q^{-1})_m} (-1)^{k+m+1} q^{-km-(k+m+1)/2}, \\ (R^{-1})_{l,m}^{j,k} &= \delta_{m,j+h} \delta_{l,k-h} \frac{(q)_j^{-1} (q)_k}{(q)_h (q)_l (q)_m^{-1}} (-1)^{j+l+1} q^{jl+(j+l+1)/2}, \end{aligned}$$

where $j, k, l, m, h \in \{0, 1, \dots, N-1\}$ and $\delta_{j,k}$ is the Kronecker's delta. If $R_{l,m}^{j,k} \neq 0$, then h is uniquely determined by the formula $h = j - m = l - k$, and if $(R^{-1})_{l,m}^{j,k} \neq 0$, then $h = m - j = k - l$.

Note that this R-matrix is the inverse of the one in [7]. This implies the colored Jones polynomial of a knot K here is the one of the mirror image \overline{K} in [7]. This choice is more natural to [16] and Theorem 1.3.

Let K be the hyperbolic knot with a fixed diagram and G be the diagram defined in Section 2.1 with the orientation from J to I . We assign 0 to one bounded region of G , and then assign variables $r_1, \dots, r_m \in \{0, 1, \dots, N-1\}$ to the other bounded regions of G and $r_{m+1} \in \{0, 1, \dots, N-1\}$ to the unbounded region. We assign variables to each sides according to the signed sum of variables of adjacent regions with orientations modulo N . (See Figure 23 for an example.)

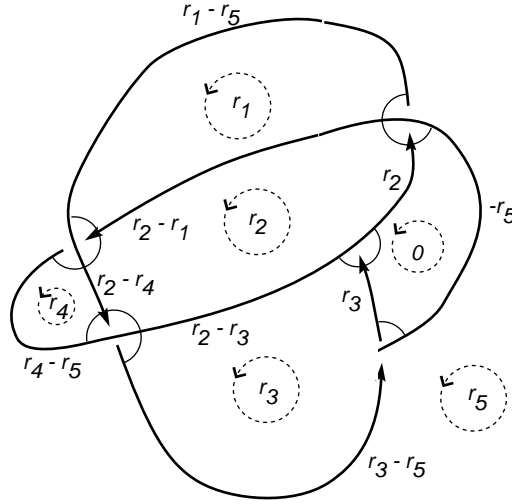


Figure 23: Assigning variables on each regions and sides

For each non-trivalent vertex of G , we assign the R-matrix to the positive crossing and the inverse to the negative crossing. Then we apply the formal substitution (1) to each R-matrix and substitute q^{r_n} to w_n as below. In the substitution process, if $r_n = 0$ then we put $w_n = 1$. Note that we apply the same R-matrix or its inverse in different forms according to the position of the collapsed horizontal edge. If none of the horizontal edges is collapsed in the octahedron, then we choose any formal substitution among the four possibilities. For positive crossings :

$$\begin{array}{c}
r_l - r_m \quad r_k - r_l \\
\quad \quad \quad r_l \\
\quad \quad \quad \diagdown \quad \diagup \\
r_m \quad \quad r_k \\
\quad \quad \quad r_j \\
\quad \quad \quad \diagdown \quad \diagup \\
r_j - r_m \quad r_k - r_j
\end{array}
: \frac{(q)_{r_l - r_m} (q^{-1})_{r_k - r_l}^{-1}}{(q)_{r_j + r_l - r_k - r_m} (q^{-1})_{r_j - r_m}^{-1} (q)_{r_k - r_j}} (-1)^{r_l + r_j + 1} \\
\times q^{(r_m - r_j)(r_k - r_j) - (2r_k - r_l - r_j + 1)/2} \\
\sim \exp \left\{ \frac{N}{2\pi i} \left(-\text{Li}_2\left(\frac{w_l}{w_m}\right) - \text{Li}_2\left(\frac{w_l}{w_k}\right) + \text{Li}_2\left(\frac{w_j w_l}{w_k w_m}\right) + \text{Li}_2\left(\frac{w_m}{w_j}\right) + \text{Li}_2\left(\frac{w_k}{w_j}\right) - \frac{\pi^2}{6} + \log \frac{w_m}{w_j} \log \frac{w_k}{w_j} \right) \right\},$$

$$\begin{array}{c}
r_l - r_m \quad r_k - r_l \\
\quad \quad \quad r_l \\
\quad \quad \quad \diagdown \quad \diagup \\
r_m \quad \quad r_k \\
\quad \quad \quad r_j \\
\quad \quad \quad \diagdown \quad \diagup \\
r_j - r_m \quad r_k - r_j
\end{array}
: \frac{(q^{-1})_{r_l - r_m} (q^{-1})_{r_k - r_l}^{-1}}{(q^{-1})_{r_j + r_l - r_k - r_m} (q^{-1})_{r_j - r_m}^{-1} (q^{-1})_{r_k - r_j}} (-1)^{r_l + r_j + 1} \\
\times q^{-(r_k - r_l)(r_k - r_j) - (2r_k - r_l - r_j + 1)/2} \\
\sim \exp \left\{ \frac{N}{2\pi i} \left(\text{Li}_2\left(\frac{w_m}{w_l}\right) - \text{Li}_2\left(\frac{w_l}{w_k}\right) - \text{Li}_2\left(\frac{w_k w_m}{w_j w_l}\right) + \text{Li}_2\left(\frac{w_m}{w_j}\right) - \text{Li}_2\left(\frac{w_j}{w_k}\right) + \frac{\pi^2}{6} - \log \frac{w_k}{w_l} \log \frac{w_k}{w_j} \right) \right\},$$

$$\begin{array}{c}
r_l - r_m \quad r_k - r_l \\
\quad \quad \quad r_l \\
\quad \quad \quad \diagdown \quad \diagup \\
r_m \quad \quad r_k \\
\quad \quad \quad r_j \\
\quad \quad \quad \diagdown \quad \diagup \\
r_j - r_m \quad r_k - r_j
\end{array}
: \frac{(q^{-1})_{r_l - r_m} (q)_{r_k - r_l}^{-1}}{(q)_{r_j + r_l - r_k - r_m} (q)_{r_j - r_m}^{-1} (q^{-1})_{r_k - r_j}} (-1)^{r_l + r_j + 1} \\
\times q^{(r_m - r_l)(r_k - r_l) - (2r_k - r_l - r_j + 1)/2} \\
\sim \exp \left\{ \frac{N}{2\pi i} \left(\text{Li}_2\left(\frac{w_m}{w_l}\right) + \text{Li}_2\left(\frac{w_k}{w_l}\right) + \text{Li}_2\left(\frac{w_j w_l}{w_k w_m}\right) - \text{Li}_2\left(\frac{w_j}{w_m}\right) - \text{Li}_2\left(\frac{w_j}{w_k}\right) - \frac{\pi^2}{6} + \log \frac{w_m}{w_l} \log \frac{w_k}{w_l} \right) \right\},$$

$$\begin{array}{c}
r_l - r_m \quad r_k - r_l \\
\quad \quad \quad r_l \\
\quad \quad \quad \diagdown \quad \diagup \\
r_m \quad \quad r_k \\
\quad \quad \quad r_j \\
\quad \quad \quad \diagdown \quad \diagup \\
r_j - r_m \quad r_k - r_j
\end{array}
: \frac{(q)_{r_l - r_m} (q)_{r_k - r_l}^{-1}}{(q^{-1})_{r_j + r_l - r_k - r_m} (q)_{r_j - r_m}^{-1} (q)_{r_k - r_j}} (-1)^{r_l + r_j + 1} \\
\times q^{-(r_m - r_l)(r_m - r_j) - (r_l + r_j - 2r_m + 1)/2} \\
\sim \exp \left\{ \frac{N}{2\pi i} \left(-\text{Li}_2\left(\frac{w_l}{w_m}\right) + \text{Li}_2\left(\frac{w_k}{w_l}\right) - \text{Li}_2\left(\frac{w_k w_m}{w_j w_l}\right) - \text{Li}_2\left(\frac{w_j}{w_m}\right) + \text{Li}_2\left(\frac{w_k}{w_j}\right) + \frac{\pi^2}{6} - \log \frac{w_m}{w_l} \log \frac{w_m}{w_j} \right) \right\}.$$

For negative crossings :

$$\begin{array}{c}
r_l - r_m \quad r_k - r_l \\
\quad \quad \quad r_l \\
\quad \quad \quad \diagdown \quad \diagup \\
r_m \quad \quad r_k \\
\quad \quad \quad r_j \\
\quad \quad \quad \diagdown \quad \diagup \\
r_j - r_m \quad r_k - r_j
\end{array}
: \frac{(q)_{r_l - r_m}^{-1} (q^{-1})_{r_k - r_l}}{(q^{-1})_{r_k + r_m - r_j - r_l} (q^{-1})_{r_j - r_m} (q)_{r_k - r_j}^{-1}} (-1)^{r_l + r_j + 1} \\
\times q^{-(r_j - r_m)(r_j - r_k) + (r_l + r_j - 2r_m + 1)/2} \\
\sim \exp \left\{ \frac{N}{2\pi i} \left(\text{Li}_2\left(\frac{w_l}{w_m}\right) + \text{Li}_2\left(\frac{w_l}{w_k}\right) - \text{Li}_2\left(\frac{w_j w_l}{w_k w_m}\right) - \text{Li}_2\left(\frac{w_m}{w_j}\right) - \text{Li}_2\left(\frac{w_k}{w_j}\right) + \frac{\pi^2}{6} - \log \frac{w_j}{w_m} \log \frac{w_j}{w_k} \right) \right\},$$

$$\begin{aligned}
& \begin{array}{c} r_l - r_m \quad r_k - r_l \\ \quad \quad r_l \\ \quad \swarrow \quad \searrow \\ r_m \quad \quad r_k \\ \quad \swarrow \quad \searrow \\ r_j - r_m \quad r_k - r_j \end{array} : \frac{(q^{-1})_{r_l - r_m}^{-1} (q^{-1})_{r_k - r_l}}{(q)_{r_k + r_m - r_j - r_l} (q^{-1})_{r_j - r_m} (q^{-1})_{r_k - r_j}^{-1}} (-1)^{r_l + r_j + 1} \\
& \quad \times q^{(r_l - r_k)(r_j - r_k) + (2r_k - r_l - r_j + 1)/2} \\
& \sim \exp \left\{ \frac{N}{2\pi i} \left(-\text{Li}_2\left(\frac{w_m}{w_l}\right) + \text{Li}_2\left(\frac{w_l}{w_k}\right) + \text{Li}_2\left(\frac{w_k w_m}{w_j w_l}\right) - \text{Li}_2\left(\frac{w_m}{w_j}\right) + \text{Li}_2\left(\frac{w_j}{w_k}\right) - \frac{\pi^2}{6} + \log \frac{w_l}{w_k} \log \frac{w_j}{w_k} \right) \right\}, \\
& \begin{array}{c} r_l - r_m \quad r_k - r_l \\ \quad \quad r_l \\ \quad \swarrow \quad \searrow \\ r_m \quad \quad r_k \\ \quad \swarrow \quad \searrow \\ r_j - r_m \quad r_k - r_j \end{array} : \frac{(q^{-1})_{r_l - r_m}^{-1} (q)_{r_k - r_l}}{(q^{-1})_{r_k + r_m - r_j - r_l} (q)_{r_j - r_m} (q^{-1})_{r_k - r_j}^{-1}} (-1)^{r_l + r_j + 1} \\
& \quad \times q^{-(r_l - r_m)(r_l - r_k) + (r_l + r_j - 2r_m + 1)/2} \\
& \sim \exp \left\{ \frac{N}{2\pi i} \left(-\text{Li}_2\left(\frac{w_m}{w_l}\right) - \text{Li}_2\left(\frac{w_k}{w_l}\right) - \text{Li}_2\left(\frac{w_j w_l}{w_k w_m}\right) + \text{Li}_2\left(\frac{w_j}{w_m}\right) + \text{Li}_2\left(\frac{w_j}{w_k}\right) + \frac{\pi^2}{6} - \log \frac{w_l}{w_m} \log \frac{w_l}{w_k} \right) \right\}, \\
& \begin{array}{c} r_l - r_m \quad r_k - r_l \\ \quad \quad r_l \\ \quad \swarrow \quad \searrow \\ r_m \quad \quad r_k \\ \quad \swarrow \quad \searrow \\ r_j - r_m \quad r_k - r_j \end{array} : \frac{(q)_{r_l - r_m}^{-1} (q)_{r_k - r_l}}{(q)_{r_k + r_m - r_j - r_l} (q)_{r_j - r_m} (q)_{r_k - r_j}^{-1}} (-1)^{r_l + r_j + 1} \\
& \quad \times q^{(r_l - r_m)(r_j - r_m) + (r_l + r_j - 2r_m + 1)/2} \\
& \sim \exp \left\{ \frac{N}{2\pi i} \left(\text{Li}_2\left(\frac{w_l}{w_m}\right) - \text{Li}_2\left(\frac{w_k}{w_l}\right) + \text{Li}_2\left(\frac{w_k w_m}{w_j w_l}\right) + \text{Li}_2\left(\frac{w_j}{w_m}\right) - \text{Li}_2\left(\frac{w_k}{w_j}\right) - \frac{\pi^2}{6} + \log \frac{w_l}{w_m} \log \frac{w_j}{w_m} \right) \right\}.
\end{aligned}$$

For the trivalent vertices of G , we assign 0 to the sides in I or J and then apply the same formal substitution to the R-matrix as follows. (In here, we do not concern the collapsing of the horizontal edges of the octahedron.)

For the end point of I :

$$\begin{aligned}
& \begin{array}{c} r_l - r_m \quad r_j - r_l \\ \quad \quad r_l \\ \quad \swarrow \quad \searrow \\ r_m \quad \quad r_j \\ \quad \swarrow \quad \searrow \\ r_j - r_m \quad 0 \end{array} : \frac{(q^{-1})_{r_j - r_m}}{(q^{-1})_{r_j - r_l}} (-1)^{r_l + r_j + 1} q^{-(r_j - r_l + 1)/2} \\
& \sim \exp \left\{ \frac{N}{2\pi i} \left(\text{Li}_2\left(\frac{w_m}{w_j}\right) - \text{Li}_2\left(\frac{w_l}{w_j}\right) \right) \right\}, \\
& \begin{array}{c} r_l - r_j \quad r_k - r_l \\ \quad \quad r_l \\ \quad \swarrow \quad \searrow \\ r_j \quad \quad r_k \\ \quad \swarrow \quad \searrow \\ 0 \quad r_j \quad r_k - r_j \end{array} : \frac{(q)_{r_k - r_j}}{(q)_{r_l - r_j}} (-1)^{r_l + r_j + 1} q^{(r_l - r_j - 1)/2} \\
& \sim \exp \left\{ \frac{N}{2\pi i} \left(-\text{Li}_2\left(\frac{w_k}{w_j}\right) + \text{Li}_2\left(\frac{w_l}{w_j}\right) \right) \right\}.
\end{aligned}$$

For the end point of J :

$$\begin{array}{c}
\begin{array}{ccc}
r_k - r_m & & 0 \\
& \searrow & \nearrow \\
r_m & & r_k \\
& \swarrow & \searrow \\
r_j - r_m & & r_k - r_j
\end{array} \\
\end{array}
\begin{array}{l}
: \frac{(q^{-1})_{r_k - r_m}}{(q^{-1})_{r_k - r_j}} (-1)^{r_k + r_j + 1} q^{-(r_k - r_j + 1)/2} \\
\sim \exp \left\{ \frac{N}{2\pi i} \left(\text{Li}_2\left(\frac{w_m}{w_k}\right) - \text{Li}_2\left(\frac{w_j}{w_k}\right) \right) \right\},
\end{array}$$

$$\begin{array}{c}
\begin{array}{ccc}
0 & & r_k - r_l \\
& \swarrow & \searrow \\
& & r_l \\
& \swarrow & \searrow \\
r_j - r_l & & r_k - r_j
\end{array} \\
\end{array}
\begin{array}{l}
: \frac{(q)_{r_k - r_l}}{(q)_{r_j - r_l}} (-1)^{r_l + r_j + 1} q^{(r_j - r_l + 1)/2} \\
\sim \exp \left\{ \frac{N}{2\pi i} \left(-\text{Li}_2\left(\frac{w_k}{w_l}\right) + \text{Li}_2\left(\frac{w_j}{w_l}\right) \right) \right\}.
\end{array}$$

Note that the colored Jones polynomial is expressed by the products of various forms of the R-matrices of crossings or trivalent vertices of G (with slight modification by the local maxima/minima) and take summation over all the possible indices r_1, \dots, r_{m+1} . (See [7] for the calculation of the colored Jones polynomial. The description in [7] may look slightly different from ours, but removing the sides of the tangle diagram assigned with 0 in [7] gives the diagram G .) Now we define a potential function $\widetilde{W}(w_1, \dots, w_{m+1})$ of the knot diagram by letting the product of all formal substitutions of G to be $\exp \left\{ \frac{N}{2\pi i} \widetilde{W}(w_1, \dots, w_{m+1}) \right\}$. One important property of \widetilde{W} is that the variable w_{m+1} assigned to the unbounded region appears only in the numerator. Therefore, we can define another potential function $W(w_1, \dots, w_m) := \widetilde{W}(w_1, \dots, w_m, 0)$,¹³ which coincides with the potential function $W(w_1, \dots, w_m)$ defined in Section 3.2.

For example, \widetilde{W} and W of Figure 23 become

$$\begin{aligned}
\widetilde{W}(w_1, \dots, w_5) = & \left\{ \text{Li}_2\left(\frac{1}{w_2}\right) - \text{Li}_2\left(\frac{w_3}{w_2}\right) \right\} + \left\{ \text{Li}_2\left(\frac{w_5}{w_3}\right) - \text{Li}_2\left(\frac{1}{w_3}\right) \right\} \\
& + \left\{ -\text{Li}_2\left(\frac{w_5}{w_4}\right) + \text{Li}_2\left(\frac{w_4}{w_2}\right) + \text{Li}_2\left(\frac{w_5 w_2}{w_4 w_3}\right) - \text{Li}_2\left(\frac{w_5}{w_3}\right) + \text{Li}_2\left(\frac{w_3}{w_2}\right) - \frac{\pi^2}{6} + \log \frac{w_4}{w_2} \log \frac{w_3}{w_2} \right\} \\
& + \left\{ -\text{Li}_2\left(\frac{w_5}{w_1}\right) + \text{Li}_2\left(\frac{w_1}{w_2}\right) + \text{Li}_2\left(\frac{w_5 w_2}{w_1 w_4}\right) - \text{Li}_2\left(\frac{w_5}{w_4}\right) + \text{Li}_2\left(\frac{w_4}{w_2}\right) - \frac{\pi^2}{6} + \log \frac{w_1}{w_2} \log \frac{w_4}{w_2} \right\} \\
& + \left\{ -\text{Li}_2(w_5) + \text{Li}_2\left(\frac{1}{w_2}\right) + \text{Li}_2\left(\frac{w_5 w_2}{w_1}\right) - \text{Li}_2\left(\frac{w_5}{w_1}\right) + \text{Li}_2\left(\frac{w_1}{w_2}\right) - \frac{\pi^2}{6} + \log \frac{1}{w_2} \log \frac{w_1}{w_2} \right\},
\end{aligned}$$

and

$$\begin{aligned}
W(w_1, \dots, w_4) = & 2 \left\{ \text{Li}_2\left(\frac{1}{w_2}\right) + \text{Li}_2\left(\frac{w_4}{w_2}\right) + \text{Li}_2\left(\frac{w_1}{w_2}\right) \right\} - \text{Li}_2\left(\frac{1}{w_3}\right) - \frac{\pi^2}{2} \\
& + \log \frac{w_4}{w_2} \log \frac{w_3}{w_2} + \log \frac{w_1}{w_2} \log \frac{w_4}{w_2} + \log \frac{1}{w_2} \log \frac{w_1}{w_2}.
\end{aligned}$$

This potential function $W(w_1, \dots, w_4)$ coincides with the one defined previously in (5).

¹³Note that $\text{Li}_2(0) = 0$.

Note that using W instead of \widetilde{W} does not violate the formulation of the optimistic limit because, for a solution $(w_1^{(0)}, \dots, w_m^{(0)})$ of $\mathcal{H}_2 = \left\{ \exp \left(w_l \frac{\partial W}{\partial w_l} \right) = 1 \mid l = 1, \dots, m \right\}$, $(w_1^{(0)}, \dots, w_m^{(0)}, 0)$ becomes a solution of $\widetilde{\mathcal{H}}_2 := \left\{ \exp \left(w_l \frac{\partial \widetilde{W}}{\partial w_l} \right) = 1 \mid l = 1, \dots, m+1 \right\}$. We are considering only the solutions of $\widetilde{\mathcal{H}}_2$ with the condition $w_{m+1} = 0$ because this condition corresponds to the collapsing process of tetrahedra of Thurston triangulation in Section 2.2 and the solutions correspond to the triangulation. However, the other solutions with the condition $w_{m+1} \neq 0$ also have good geometric meanings and this will be discussed in later articles.

Acknowledgments The authors show gratitude to Yoshiyuki Yokota for sending us his preprint in advance before publication. The first author was supported by Grant-in-Aid for JSPS Fellows 21.09221, the Korea Research Foundation Grant funded by the Korean Government (KRF-2008-341-C00004) and POSCO TJ Park foundation.

References

- [1] J. Cho. Yokota theory, the invariant trace fields of hyperbolic knots and the Borel regulator map. <http://arxiv.org/abs/1005.3094>, 2010.
- [2] J. Cho and J. Murakami. The complex volumes of twist knots via colored Jones polynomials. *J. Knot Theory Ramifications*, 19(11):1401–1421, 2010.
- [3] S. Francaviglia. Hyperbolic volume of representations of fundamental groups of cusped 3-manifolds. *Int. Math. Res. Not.*, (9):425–459, 2004.
- [4] R. M. Kashaev. The hyperbolic volume of knots from the quantum dilogarithm. *Lett. Math. Phys.*, 39(3):269–275, 1997.
- [5] L. Lewin, editor. *Structural properties of polylogarithms*, volume 37 of *Mathematical Surveys and Monographs*. American Mathematical Society, Providence, RI, 1991.
- [6] R. Meyerhoff. Density of the Chern-Simons invariant for hyperbolic 3-manifolds. In *Low-dimensional topology and Kleinian groups (Coventry/Durham, 1984)*, volume 112 of *London Math. Soc. Lecture Note Ser.*, pages 217–239. Cambridge Univ. Press, Cambridge, 1986.
- [7] H. Murakami. The asymptotic behavior of the colored Jones function of a knot and its volume. *Proceedings of ‘Art of Low Dimensional Topology VI’, edited by T. Kohno, January*, 2000.
- [8] H. Murakami. Optimistic calculations about the Witten-Reshetikhin-Turaev invariants of closed three-manifolds obtained from the figure-eight knot by integral Dehn surgeries. *Sūrikaiseikikenkyūsho Kōkyūroku*, (1172):70–79, 2000. Recent progress towards the volume conjecture (Japanese) (Kyoto, 2000).

- [9] H. Murakami. Kashaev's invariant and the volume of a hyperbolic knot after Y. Yokota. In *Physics and combinatorics 1999 (Nagoya)*, pages 244–272. World Sci. Publ., River Edge, NJ, 2001.
- [10] H. Murakami and J. Murakami. The colored Jones polynomials and the simplicial volume of a knot. *Acta Math.*, 186(1):85–104, 2001.
- [11] H. Murakami, J. Murakami, M. Okamoto, T. Takata, and Y. Yokota. Kashaev's conjecture and the Chern-Simons invariants of knots and links. *Experiment. Math.*, 11(3):427–435, 2002.
- [12] K. Ohnuki. The colored Jones polynomials of 2-bridge link and hyperbolicity equations of its complements. *J. Knot Theory Ramifications*, 14(6):751–771, 2005.
- [13] D. Thurston. Hyperbolic volume and the Jones polynomial. Lecture note at “Invariants des noeuds et de variétés de dimension 3”, available at <http://www.math.columbia.edu/~dpt/speaking/Grenoble.pdf>, June 1999.
- [14] W. Thurston. The geometry and topology of three-manifolds. Lecture Note. available at <http://www.msri.org/publications/books/gt3m/>.
- [15] S. Tillmann. Degenerations of ideal hyperbolic triangulations. <http://arxiv.org/abs/math/0508295>.
- [16] Y. Yokota. On the volume conjecture for hyperbolic knots. <http://arxiv.org/abs/math/0009165>.
- [17] Y. Yokota. On the complex volume of hyperbolic knots. *J. Knot Theory Ramifications*, 20(7):955–976, 2011.
- [18] C. K. Zickert. The volume and Chern-Simons invariant of a representation. *Duke Math. J.*, 150(3):489–532, 2009.

SCHOOL OF MATHEMATICS, KOREA INSTITUTE FOR ADVANCED STUDY, 85 HOEGIRO,
DONGDAEMUN-GU, SEOUL 130-722, REPUBLIC OF KOREA

DEPARTMENT OF MATHEMATICS, FACULTY OF SCIENCE AND ENGINEERING, WASEDA
UNIVERSITY, 3-4-1 OKUBO, SHINJUKU-KU, TOKYO 169-8555, JAPAN

E-MAIL: DOL0425@GMAIL.COM

MURAKAMI@WASEDA.JP